



DeepSeek-VL: Towards Real-World Vision-Language Understanding

Haoyu Lu^{*1†}, Wen Liu^{*1}, Bo Zhang^{*1‡}, Bingxuan Wang^{1†}, Kai Dong¹, Bo Liu^{1†}, Jingxiang Sun^{1†}, Tongzheng Ren^{1†}, Zhusuo Li¹, Hao Yang^{1†}, Yaofeng Sun¹, Chengqi Deng¹, Hanwei Xu¹, Zhenda Xie¹, Chong Ruan¹

¹DeepSeek-AI

{neal, liuwen, bo}@deepseek.com

<https://github.com/deepseek-ai/DeepSeek-VL>

Abstract

We present DeepSeek-VL, an open-source Vision-Language (VL) Model designed for real-world vision and language understanding applications. Our approach is structured around three key dimensions:

- **Data Construction:** We strive to ensure our data is diverse, scalable and extensively covers real-world scenarios including web screenshots, PDFs, OCR, charts, and knowledge-based content (expert knowledge, textbooks), aiming for a comprehensive representation of practical contexts. Further, we create a use case taxonomy from real user scenarios and construct an instruction-tuning dataset accordingly. The fine-tuning with this dataset substantially improves the model’s user experience in practical applications.

- **Model Architecture:** Considering efficiency and the demands of most real-world scenarios, DeepSeek-VL incorporates a hybrid vision encoder that efficiently processes high-resolution images (1024 x 1024) within a fixed token budget, while maintaining a relatively low computational overhead. This design choice ensures the model’s ability to capture critical semantic and detailed information across various visual tasks.

- **Training Strategy:** We posit that a proficient Vision-Language Model should, foremost, possess strong language abilities. To ensure the preservation of LLM capabilities during pretraining, we investigate an effective VL pretraining strategy by integrating LLM training from the beginning and carefully managing the competitive dynamics observed between vision and language modalities. Starting with a focus on text, we gradually adjust the ratio to facilitate a balanced integration of both modalities.

The DeepSeek-VL family (both 1.3B and 7B models) showcases superior user experiences as a vision-language chatbot in real-world applications, achieving state-of-the-art or competitive performance across a wide range of visual-language benchmarks at the same model size while maintaining robust performance on language-centric benchmarks. We have made both 1.3B and 7B models publicly accessible to foster innovations based on this foundation model.

^{*} Equal contribution.

[†] Work done during the internship at DeepSeek-AI.

[‡] Project lead.

Contents

1	Introduction	3
2	Data Construction	6
2.1	Vision-Language pretraining Data	6
2.2	Supervised Fine-tuning Data	8
3	Approach	10
3.1	Architecture	10
3.2	Training Pipelines	12
3.2.1	Stage 1: Training Vision-Language Adaptor	12
3.2.2	Stage 2: Joint Vision-Language pretraining	13
3.2.3	Stage 3: Supervised Fine-tuning	14
3.3	Hyperparameters and Infrastructures	15
4	Evaluation	16
4.1	Public Multimodal Benchmarks Evaluation	16
4.2	Public Language Benchmarks Evaluation	17
4.3	Human Evaluation	18
4.4	Ablation Study	19
5	Conclusion, Limitation, and Future Work	22
A	Appendix	30

1. Introduction

The remarkable success of large language models (LLMs) ([Anthropic, 2023](#); [Google, 2023](#); [OpenAI, 2022, 2023a](#)) has fueled the demand for a versatile interface that can handle multiple modalities beyond language. In response to this growing demand, we have seen an emergence of Large Multimodal Models (LMMs) like GPT-4V ([OpenAI, 2023b](#)) and Gemini ([Team et al., 2023](#)), which serve as versatile assistants capable of comprehending and acting upon instructions that span vision and language. These models exhibit considerable promise in executing complex, diverse real-world tasks, enabling more natural and human-like interactions.

Recently, there has been a surge of open-source large multimodal models aimed at narrowing the gap with proprietary counterparts. Substantial strides have been made, especially in benchmark performance, yet a significant divide persists between the majority of open-source models and state-of-the-art closed-source models ([Bai et al., 2023](#); [Bavishi et al., 2023](#); [OpenAI, 2023b](#); [Team et al., 2023](#)) when it comes to real-world performance and user experience. It remains challenging for the open-source community to develop models with robust general multimodal capabilities for real-world applications.

The performance gap between the most open-source models and the proprietary models is largely pronounced in real-world scenarios, primarily due to the following reasons:

- Many open-source solutions allocate a significant proportion of computational resources to the instruction tuning phase. However, the experience of training powerful language models underscores the importance of extensive pretraining in the development of general intelligence. To imbue multimodal models with rich world knowledge, there should be an emphasis on comprehensive pretraining that leverages a broad spectrum of vision-language data.
- A common practice is to amalgamate various academic datasets during instruction tuning. While such an approach may yield good benchmark results, it often falls short in providing an authentic real-world usage experience.
- In terms of model architecture, prior works mostly adapt a vision transformer, typically text-aligned, to a pre-trained language model. However, most of these models operate on a relatively low resolution, e.g., 336×336 or 448×448 . The intricacies of complex real-world scenarios, such as optical character recognition or tiny object discernment, demand high-resolution processing capability.
- While some models ([01-ai, 2024](#); [Lin et al., 2023a](#); [Sun et al., 2023](#); [Wang et al., 2023b](#)) have begun to exploit pretraining, they often overlook the preservation of language skills. Often, there is a degradation of language capability after prolonged multimodal training. Since we aim for a generalist that possesses strong capabilities in both modalities, there should be a training strategy that well preserves the language capability when developing the new modality ability.

In light of these, we present DeepSeek-VL, an open-source large multimodal model, which is built upon the DeepSeek language model series. We develop the model in the pursuit of adept performance in real-world scenarios, which involves extensive pretraining, careful data curation based on a use case taxonomy, model architecture design for high-resolution processing, and a training strategy that balances the multi-modalities. On top of these, we develop a training methodology that steers the model scaling, from 1B to 7B. These comprehensive explorations bring a significant performance advantage in practical settings, compared to other large multimodal models (LMMs) of similar size.

The diagram illustrates the workflow of the proposed approach:

- (1) Create dataset pre-training:** An image is processed by an **Image Extractor** to produce a feature vector (b_1, b_2, \dots, b_n). This vector is then used by a **Linear Predictor** to predict a class label (y_1, y_2, \dots, y_n).
- (2) Create dataset classifier:** A **Feature Extractor** takes the same image and produces a feature vector (b_1, b_2, \dots, b_n). This vector is used by a **Linear Predictor** to predict a class label (y_1, y_2, \dots, y_n).
- (3) Use semi-supervised prediction:** An image is processed by an **Image Extractor** to produce a feature vector (b_1, b_2, \dots, b_n). This vector is used by a **Linear Predictor** to predict a class label (y_1, y_2, \dots, y_n).

 **Response**

图片展示了一个名为CLIP的算法的流程图。该算法被描述为一种新的零样本图像到图像转换方法，它使用文本描述来预测目标数据集的类。在流程图中，我们看到了三个主要步骤：

1. **Contrastive pre-training (对比式预训练)**：在这个阶段，模型被训练以最小化两个编码器之间的差异，一个用于图像，另一个用于文本。这通过将图像和文本嵌入投影到相同的潜在空间中来实现。
2. **Create dataset classifier from label text (创建标签文本分类器)**：这个步骤涉及从给定的标签文本中提取特征向量，并将其与图像嵌入一起输入到一个分类器中。
3. **Use for zero-shot prediction (用于零样本文本预测)**：最后，使用前面步骤中学习的模型进行零样本文本预测。这涉及到将图像嵌入和提取的特征向量传递给分类器，以预测图像属于哪个类别。

整个过程都围绕着学习一个能够理解图像和文本之间关系的模型这一核心概念。这种方法的关键在于利用大量的无标注数据，通过对比式的预训练来提高模型的泛化能力。在流程图的底部，有一个例子展示了如何使用该方法在零样本情况下识别一只鸟。

A modern kitchen interior featuring white cabinetry, a large island with a granite countertop, and two large pendant lights hanging over the island. The kitchen is well-lit with recessed ceiling lights.

 **Response**

To fetch something from the fridge, I would follow these steps:

Approach the refrigerator: The refrigerator is located on the right side of the kitchen island. It's a stainless steel model with a freezer compartment at the bottom and an ice maker dispense above it.

Open the refrigerator door: To open the refrigerator door, I would use my hands to grasp the handle or pull bar located on the front edge of the refrigerator door. This action should be done carefully to avoid any accidental bumps into other items in the kitchen.

Locate the desired item: Once inside the refrigerator, I would scan through the shelves and compartments for the specific item I am looking for. The refrigerator has multiple shelves and drawers that are likely organized by type of food or drink.

Retrieve the item: After locating the desired item, I would reach out and grab it using one hand while ensuring not to disturb the organization of the contents. If the item is placed on a shelf or drawer, I would lift it up gently to remove it without knocking anything over.

The floor plan illustrates a spacious apartment layout. It features three bedrooms: bedroom A (top left), bedroom B (top right), and bedroom C (bottom right). Three bathrooms are also present: bathroom A (bottom left), bathroom B (middle right), and bathroom C (bottom right). The layout includes a large open-plan living and dining area with a central kitchen. There are multiple walk-in closets (WIC) indicated by small arrows pointing to specific wall locations. The plan also shows several windows and doors, including a main entrance door at the bottom center.

样本预测。这里，一张狗的照片和一个关于狗的短语被用来自预测这张照片中的狗属于哪个品种。

总的来说，流程图清晰地描绘了CLIP算法的结构和它的工
作原理，强调了它在处理大量未标记数据方面的潜力以及
其对零样本任务的有效性。

 **Response**

Bedroom A is closer to Bathroom A.
This can be determined by observing the floor plan provided in the image. The layout of the rooms and bathrooms are clearly marked with labels, allowing us to identify their relative positions. Bedroom A is located on the left side of the floor plan, while Bathroom A is situated directly below it, towards the bottom-left corner of the image. This positioning indicates that there is no other bathroom between them, making Bathroom A the closest one for Bedroom A.

 **Response**

The flowchart provided is a simple decision-making process

Prompt

Tell me the main contribution of this paper.

The role of individual differences in human automated vehicle interaction

Christopher K. Fultz^{1,2}, Megan M. Meritt¹, Christopher A. Stevens³, Garrett Dean⁴

¹College of Optical Sciences, University of Arizona, Tucson, AZ, United States
²College of Optical Sciences, University of Arizona, Tucson, AZ, United States
³University Advanced Research, University of Arizona, Tucson, AZ, United States
⁴College of Optical Sciences, University of Arizona, Tucson, AZ, United States

ARTICLE INFO

Keywords: Driver behavior; Individual differences; Cognitive abilities; Cognitive load

ABSTRACT

An analysis is conducted on cognitive load theory, acknowledging how human interact with these new technologies. The purpose of this study is to examine the relationship between cognitive load and driver performance. Specifically, we hypothesize that lower automated vehicle interaction and related risk assessment, will reduce driver cognitive load, which will result in better driver performance. We describe several methods used to measure individual differences in cognitive load and their relationship to driver performance. We also describe the relationship between cognitive load and driving effects on cognitive interactions. Finally, we are on a mission to determine possible benefits of creating automated vehicles.

1. Introduction

New technologies are developed with the intention of solving critical problems and making user impacts of this nature. As a result, there is a need to understand how these technologies affect drivers' safety, which require more time and attention. In addition, as these technologies become more advanced, they will continue to change the way drivers think and understand processes, but also provide increased complexity. This study is focused on the cognitive load of drivers interacting with automated vehicles. Specifically, we hypothesize that cognitive load in high status domains such as automated vehicle interaction will be reduced, which will result in better driver performance. Investigating interactions with an automated vehicle may be a key to understanding how drivers interact with these technologies and the risk or decreasing status interactions (Hollingshead, 1995). Specifically, we hypothesize that cognitive load will be reduced when an automated vehicle interacts with drivers, as compared to the time it takes to learn to interact with a vehicle (Fultz et al., 2012; 2016). Specifically, we hypothesize that cognitive load will be reduced when an automated vehicle interacts with drivers, as compared to the time it takes to learn to interact with a vehicle (Fultz et al., 2012; 2016). Specifically, we hypothesize that cognitive load will be reduced when an automated vehicle interacts with drivers, as compared to the time it takes to learn to interact with a vehicle (Fultz et al., 2012; 2016).

Identifying individual differences in cognitive load and related risk assessment is important to understand and reduce the potential risks associated with the use of automated vehicles and new technology. This is particularly true for the human-automated vehicle interaction, as the driver's cognitive load may serve as a predictor of automated passenger vehicle. Cognitive models may serve as useful tools for understanding performance in human-automated vehicle interaction. A cognitive model is a computational or mathematical representation of a cognitive process or system that attempts to explain how people think and act (Feldman & Markman, 1996). Specifically, cognitive models are used to represent knowledge, reasoning, and computation—the neural and cognitive processes that underlie complex mental functions such as language comprehension, memory, and problem solving. These models can be used to predict cognitive performance—by physical simulation or by direct comparison with human performance. Research methods, namely, memory explicit, and cognitive load are used to identify the cognitive load of drivers interacting with automated vehicles. Specifically, we hypothesize that cognitive load will be reduced when an automated vehicle interacts with drivers, as compared to the time it takes to learn to interact with a vehicle (Fultz et al., 2012; 2016). Moreover, a cognitive model can be used to identify specific types of cognitive load that are associated with the interaction of drivers with automated vehicles. Specifically, we hypothesize that cognitive load will be reduced when an automated vehicle interacts with drivers, as compared to the time it takes to learn to interact with a vehicle (Fultz et al., 2012; 2016).

In order to identify specific types of cognitive load that are associated with the interaction of drivers with automated vehicles, we hypothesize that cognitive load will be reduced when an automated vehicle interacts with drivers, as compared to the time it takes to learn to interact with a vehicle (Fultz et al., 2012; 2016).

Our central idea is that the increasing individual differences in cognitive load will be largest for those individuals who have

 **Response**

The main contribution of this paper, as stated in the abstract, is to develop a cognitive model that integrates individual differences into human-automated vehicle interaction. The authors aim to provide insights into how humans interact with new technologies and propose a framework for understanding these interactions. They also discuss potential pitfalls associated with using a one-size-fits-all model and explain how modeling individual differences can help design effective user interfaces and interventions. Additionally, they conduct a simulation study to demonstrate possible benefits from incorporating individual differences into the design process. This conclusion is drawn directly from the text under the "ABSTRACT" section, where it outlines the purpose and contributions of the research.

Prompt

Can you translate the flowchart to a python code?

```

graph TD
    Start([Start]) --> GetX[x = Get next input]
    GetX --> GetY[y = Get next input]
    GetY --> Decision{X > Y?}
    Decision -- TRUE --> MaxX[max = x]
    MaxX --> PutMax[Put max to output]
    PutMax --> End([End])
    Decision -- FALSE --> MaxY[max = y]
    MaxY --> PutMax
  
```

The flowchart starts with an initial state. It then enters a loop where it gets the next input for variable x . It then gets the next input for variable y . It compares x and y . If $x > y$, it sets $max = x$; otherwise, it sets $max = y$. Finally, it puts max to output and ends.

that compares two variables, x and y , to determine which one has the greater value. The steps are as follows:

1. Start with an input for variable ' x ' and get its next input.
2. Repeat step 1 for variable ' y '.
3. Compare ' x ' and ' y ' using the ' $x > y$ ' condition. If true, it means ' x ' is greater than ' y ', so put the maximum of these two values into the output. If false, it means ' x ' is not greater than ' y ', so put the maximum of ' x ' and ' y ' into the output.
4. Finally, end the program by putting the max value into the output.

Here is how you can translate this flowchart into Python code:

```

def max_of_two(x, y):
    # Step 3: compare x and y
    if x > y:
        # Step 4: if x is greater than y, output max = x
        return x
    else:
        # Step 5: if x is not greater than y, output max = y
        return y

# Put max to output
output = max_of_two(input_value_for_x, input_value_for_y)
print(output)

```

In this Python code, we define a function called `max_of_two` that takes two arguments, x and y , and returns the maximum of these two values. We then call this function with the

A screenshot of the official Minecraft website. The top features a large green banner with the text "WELCOME TO THE OFFICIAL SITE OF MINECRAFT". Below the banner, a subtext reads: "With new games, new updates, and new ways to play, join one of the biggest communities in gaming and start crafting today!" A prominent green button labeled "GET MINECRAFT" is centered. The background shows a scenic view of a Minecraft landscape with a wooden house, a pool, and two characters standing on a cliff edge. The bottom of the page has a white footer bar.

A screenshot of the official Minecraft website. The top navigation bar includes links for "HOME", "ABOUT", "PLAY", "CREATE", "MODS", "NEWS", and "FORUMS". Below the navigation is a large, stylized "Minecraft" logo. The main content area features a large, colorful image of a Minecraft landscape with a village, a forest, and a body of water under a blue sky with white clouds. To the left of the image, the word "Response" is written in a bold, sans-serif font. The right side of the image contains descriptive text about the game's features and its impact on the gaming community.

A painting in the Impressionist style depicting a coastal scene. The composition features large, craggy cliffs in the background, rendered with thick, textured brushstrokes in shades of green, yellow, and brown. In the foreground, several sailboats are visible on the water, their sails catching the light. The sky is filled with soft, blended colors of blue, yellow, and white, suggesting a bright, sunny day. The overall effect is one of light and atmosphere, characteristic of the Impressionist genre.

 appropriate inputs and print the result.

Response

The art style evident in this image is Impressionism. This can be determined by several visual clues present:

Brushwork: The painting exhibits a loose, visible brushstroke technique which is characteristic of Impressionist art. The strokes are not smooth or blended but rather they create a sense of movement and texture.

Color Palette: The use of bright, vibrant colors that seem to capture the light and atmosphere of the scene without precise detail is typical of Impressionist painters. The sky's blue with white clouds, the warm tones on the cliffs, and the varied hues used for the boats all contribute to this impressionistic approach.

Subject Matter: The subject matter itself—a coastal landscape with figures and boats—is common in Impressionist paintings, which often depicted scenes from daily life and nature.

Lack of Detail: There is a lack of fine detail in the depiction of objects such as the boats and figures, which suggests an emphasis on capturing the overall mood and impression of the scene rather than meticulous realism.

Light and Shadow: The play of light and shadow is another hallmark of Impressionist works. In this painting, we see how the artist has captured the interplay of sunlight on the water and rocks, creating a dynamic effect. These elements together strongly suggest that the artwork belongs to the Impressionist genre.

Validation sequence length (x 10 ³)	NoPE (orange dashed)	RoPE (teal dashed)	Alibi (red dashed)	Kerpel (magenta dashed)	FIRE (ours) (orange solid)
1	3.05	3.00	2.95	2.95	2.85
2	2.95	2.85	2.80	2.80	2.80
3	2.90	2.85	2.80	2.80	2.80
4	3.00	3.15	2.80	2.80	2.80
5	3.10	3.20	2.80	2.85	2.80
6	3.15	3.25	2.80	2.90	2.80
7	3.18	3.30	2.80	2.95	2.80
8	3.20	3.35	2.80	3.00	2.80

“Language modeling (large model)”, suggests that this graph pertains to a study or analysis related to large-scale natural language processing tasks, specifically focusing on language modeling using a C4 dataset.

To determine the most likely direction of paper from which the table originated, we should look for visual clues in the image:

- 1. Graph Style:** The graph has a clear and professional appearance, suggesting it could be part of an academic paper or technical report.
- 2. Data Representation:** The use of multiple lines with markers such as squares, diamonds, and circles indicates comparisons between different models or methods. This kind of data representation is common in research papers where different experimental results are presented side by side for comparison.
- 3. Title and Content:** The title provides context about the nature of the content – it mentions “language modeling” and “large model,” indicating that the paper deals with computational linguistics or machine learning topics.
- 4. Legend:** There is a legend at the bottom left that matches the colors of the lines to their respective models. This is typical in scientific graphs to help readers understand what each line represents without having to refer back to the text.
- 5. Axis Labels:** The axes have labels that are consistent with scientific notation (“Validation sequence length” and “Validation log perplexity”). These labels suggest that the paper is intended for an audience familiar with these terms, which would include researchers or students in fields like computer science or engineering.
- 6. Font and Formatting:** The font used for the title and axis labels appears to be sans-serif, which is often used in modern publications due to its readability and clean design.

Based on these observations, the most likely source of the table in the picture is a publication from a field related to artificial intelligence, machine learning, or computational linguistics. It could be a journal article, conference proceedings, a thesis, or even a presentation slide from a seminar or workshop. The style and content align well with scholarly work in those domains.

Figure 1 | DeepSeek-VL possesses general multimodal understanding capabilities, capable of processing logical diagrams, web pages, formula recognition, scientific literature, natural images, and embodied intelligence in complex scenarios.

DeepSeek-VL’s pretraining dataset is compiled from a variety of sources, including but not limited to Common Crawl, Web Code, E-books, Educational Materials, and arXiv Articles. This collection thoroughly encompasses real-world scenarios such as web screenshots, PDFs, OCR, charts, and knowledge-based content (expertise, textbooks), aiming for a broad and practical representation while remaining scalable.

While our pretraining data encompasses a wide array of world knowledge, we meticulously curate our instruction-tuning dataset to reflect real-world usage scenarios. To achieve this, we manually gather authentic test cases for GPT-4V and Gemini from the Internet. These cases have been systematically organized into a comprehensive taxonomy. We use this structured taxonomy to choose prompts for each test image, ensuring a practical and relevant instruction tuning dataset. This taxonomy is also used to create an evaluation dataset that effectively assesses real-world performance.

The visual module is designed to optimize the utilization of high-resolution visual inputs while remaining within a fixed token budget to manage inference costs effectively. As such, we employ a hybrid vision encoder, which combines a text-aligned encoder for coarse semantic extraction at 384×384 resolution with a high-resolution encoder that captures detailed visual information at 1024×1024 resolution. By fusing these two encoders, our hybrid approach efficiently condenses a 1024×1024 resolution image (which suffices in most use cases) into 576 tokens. This token count strikes a balance between rich visual representation and token economy, making it feasible for both text-image interleaving and multi-turn inference scenarios.

During the pretraining of multimodal models, a common challenge encountered is the potential degradation of language capabilities when the training process is overly reliant on vision-language data. Our research reveals that maintaining a significant proportion of language data—specifically, at least 70%—is essential to preserve the integrity of language knowledge within the model. This balance is critical for achieving a robust multimodal capability that does not compromise language performance. Moreover, we introduce a novel “modality warm-up” strategy. This approach carefully adjusts the ratio of modalities during training, gradually incorporating more vision-language data. The careful tuning of the modality ratio along with the warm-up strategy results in a balanced performance of both modalities.

When iterating on our model, We conduct experiments on a small scale before scaling to a larger model size. However, a smaller model, e.g., 1B model, cannot demonstrate reasonable performance on benchmarks ([Schaeffer et al., 2024](#)) and faithfully reflect the model’s performance. We adopt two approaches to address this. First, we modify the evaluation protocol from multi-choice to compare the perplexity of options. Also, to prevent the instruction following ability from becoming the bottleneck, we mix a small proportion of instruction tuning data during the pretraining phase. In this way, we can achieve reasonable performance using the 1B model and more accurately measure the impact of each iteration during the experiment.

Through extensive evaluations of general vision and language benchmarks, the DeepSeek-VL family showcases superior user experiences in real-world applications and achieves state-of-the-art or competitive performance across a wide range of visual-language benchmarks at the same model size, while maintaining robust language-centric performance. To foster innovation and enable a wide range of applications, we have made two versions of our ours, 1.3B and 7B, publicly accessible, in the hope of facilitating the needs of varying computational capabilities.

2. Data Construction

A diverse and large dataset is the most important ingredient of visual language model training. Our dataset can be divided into two parts: Vision-Language pretraining Data and Vision-Language Supervised Fine-Tuning Data. VL pretraining Data is composed of visual-text data from various sources, aimed at enhancing the model’s fundamental cross-modal understanding capabilities; while VL Supervised Fine-Tuning Data has a relatively smaller size and aims to teach the model to complete specific downstream tasks. By design, VL pretraining Data is used to warm up the vision-language adaptor in training stage 1 and jointly pretrain the vision-language model in stage 2, and VL Supervised Fine-Tuning Data is exploited in training stage 3, i.e., vision language supervised fine-tuning.

2.1. Vision-Language pretraining Data

The pretraining dataset utilized in our study encompasses a diverse range of publicly accessible sources, in addition to a selection of proprietary data. We provide a comprehensive overview of the data sources employed during the joint vision and language pretraining stage in Table 1. Such a dataset can facilitate LLM’s comprehension of the entities portrayed in the images.

Furthermore, we present a detailed breakdown of the complete dataset, which is organized into the following categories:

Interleaved image-text data enable the models to have a better capability for in-context learning of multi-modality inputs, and we utilize three public datasets MMC4 ([Zhu et al., 2024](#)), Wiki ([Burns et al., 2023](#)), Wikihow ([Yang et al., 2021](#)) and Epub textbooks.

Image caption data come from three high-quality image-text paired datasets: Capsfusion ([Yu et al., 2023a](#)), TaiSu ([Liu et al., 2022b](#)) and Detailed Caption ([echo840, 2024](#)).

Table and chart data enable the models to learn the capability for general table and chart image understanding. It encompasses a diverse range of public data sources, including Chart2text ([Kanthalraj et al., 2022](#)), Geo170K ([Gao et al., 2023](#)), Unichart ([Masry et al., 2023](#)), Ureader ([Ye et al., 2023](#)), M-paper ([Hu et al., 2023](#)), ScienceQA ([Lu et al., 2022b](#)), ScreenQA ([Hsiao et al., 2022](#)), SciGraphQA-295K ([Li and Tajbakhsh, 2023](#)), Paper2figure100k ([Rodriguez et al., 2023](#)), Widget Captioning ([Li et al., 2020](#)), Screen2words ([Wang et al., 2021](#)), and Refexp ([Mao et al., 2016](#)).

Web Code data empowers models with the capability to reconstruct code from graphical interfaces or visual plots. Leveraging Websight ([HuggingFaceM4, 2024](#)) for UI Inverse Rendering, we adopted a strategy akin to that used in MATCHA ([Liu et al., 2022a](#)) for visual plots inverse rendering. This involved the processing of approximately 1.46 million Jupyter notebooks from the Stack dataset ([Kocetkov et al., 2023](#)). By extracting these notebooks and collating all diagrams along with their corresponding preceding code segments, we succeeded in curating a collection featuring 2 million pairs of images and codes. For better data quality, we filter 1.1 million instances, each comprising a singular image coupled with a minimum of 5 lines of code, to constitute our primary training dataset.

Document Optical Character Recognition (OCR) data facilitates the recognition of optical characters at the document level, even in challenging real-world scenarios. To the best of our knowledge, there is currently no publicly available large-scale dataset encompassing both English and Chinese documents. Despite the existence of the publicly accessible small-scale dataset Latex-OCR ([Blecher, 2024](#)), we additionally constructed a comprehensive English and

Table 1 | Summary of datasets used in the joint vision and language pretraining stage.

Category	Dataset	Ratio
Interleaved image-text	MMC4 (Zhu et al., 2024) Wikipedia EN& CN (Foundation) Wikihow (Yang et al., 2021) in-house PDF and Epub textbooks	13.1%
Image caption	Capsfusion (Yu et al., 2023a) TaiSu (Liu et al., 2022b) Detailed Caption (echo840, 2024)	11.1%
Table and chart	Chart2text (Kanthalraj et al., 2022) Geo170K (Gao et al., 2023) Ureader (Ye et al., 2023) Unichart (Masry et al., 2023) M-paper (Hu et al., 2023) ScienceQA (Lu et al., 2022b) ScreenQA (Hsiao et al., 2022) SciGraphQA-295K (Li and Tajbakhsh, 2023) Paper2figure100k (Rodriguez et al., 2023) Widget Captioning (Li et al., 2020) Screen2words (Wang et al., 2021) Refexp (Mao et al., 2016)	2.1%
Web Code	Websight (HuggingFaceM4, 2024) python plots scraped from GitHub notebook	0.4%
Scene text OCR	ArT (Chng et al., 2019) MLT-17 (Nayef et al., 2017) LSVT (Sun et al., 2019) UberText (Zhang et al., 2017) Coco-text (Veit et al., 2016) RCTW-17 (Shi et al., 2017) ReCTS (Zhang et al., 2019) TextOCR (Singh et al., 2021) OpenVINO (Krylov et al., 2021) HierText (Long et al., 2022)	1.2%
Document OCR	arXiv rendered markdown (Blecher et al., 2023)	2.1%
Text-only corpus	DeepSeek-LLM 2T text copus (DeepSeek-AI, 2024)	70.0%

Chinese document OCR dataset. It is comprised of two parts: 1): **arXiv Articles:** We collected source code and compiled PDFs from 1.4 million arXiv articles. Utilizing pre-processing tools from Nougat ([Blecher et al., 2023](#)), we rendered these articles into paired images and texts; 2): **E-books and Educational Materials:** We cleaned 860K English and 180K Chinese e-books from Anna’s Archive ([Anna’s Archive, 2024](#)) alongside millions of K-12 education exam questions. Subsequently, we employed HTML rendering tools ([Kulkarni and Truelson](#)) to convert these HTML files with different templates into paired image and text formats.

Scene text OCR data augment the capability of the model to recognize and extract text from images in which the text is integrated into the environment. The dataset is composed of multiple

Table 2 | Summary of data used in our joint vision and language supervised fine-tuning stage.

Class	Dataset	Ratio
In-house Data	SFT data based on taxonomy (Figure 3)	10.5%
General Multi-modality	ShareGPT4V (Chen et al., 2023) LAION-GPTV (LAION, 2023) LVIS-Instruct4V (Wang et al., 2023a) textOCR-GPT4V (Carter, 2024) LLaVA1.6-GPT4V (Liu et al., 2024a) IconQA (Lu et al., 2021)	35.5%
Table and chart	Ureader (Ye et al., 2023) Geo170K (Gao et al., 2023) ScienceQA (Lu et al., 2022b)	4.1%
Web Code	Screen-to-code (Abi, 2024) ScreenQA (Hsiao et al., 2022)	2.0%
Text-only SFT	DeepSeek-LLM (DeepSeek-AI, 2024)	47.9%

public datasets, including ArT (Chng et al., 2019), MLT-17 (Nayef et al., 2017), LSVT (Sun et al., 2019), UberText (Zhang et al., 2017), Coco-text (Veit et al., 2016), RCTW-17 (Shi et al., 2017), ReCTS (Zhang et al., 2019), TextOCR (Singh et al., 2021), OpenVINO (Krylov et al., 2021) and HierText (Long et al., 2022).

Text-only corpus serves to maintain proficiency in language-centric tasks. In this study, we employ the same text corpus with DeepSeek-LLM (DeepSeek-AI, 2024).

2.2. Supervised Fine-tuning Data

The supervised fine-tuning datasets utilized in our study encompass a diverse range of multi-modality and language data sources, including well-known open-source shared gpt4v datasets such as ShareGPT4V (Chen et al., 2023), LAION-GPTV (LAION, 2023), LVIS-Instruct4V (Wang et al., 2023a), textOCR-GPT4V (Carter, 2024), LLaVA1.6-GPT4V (Liu et al., 2024a) and IconQA (Lu et al., 2021). Additionally, we incorporate partial table and chart data extracted from pretraining datasets such as Ureader (Ye et al., 2023), ScreenQA (Hsiao et al., 2022), Geo170K (Gao et al., 2023), and ScienceQA (Lu et al., 2022b). Moreover, we integrate the UI Code dataset obtained from Screen-to-code (Abi, 2024) tasks. To enhance the quality of our multi-modality SFT data, we have also curated a portion of high-quality in-house multi-modality SFT data, some of which are in the Chinese language. Our in-house instruction-tuning dataset is meticulously designed to reflect real-world usage scenarios and cover a wide range of tasks. We start by collecting a diverse set of authentic test cases for GPT-4V and Gemini from various online sources. These test cases are then carefully analyzed and organized into a comprehensive taxonomy, which encompasses multiple categories, such as recognition, conversion, analysis, reasoning, evaluation, and safety, as detailed in Table 3. This structured taxonomy serves as a guideline for selecting representative prompts for each test image, ensuring that our instruction-tuning dataset is both practical and relevant to real-world applications. Moreover, this taxonomy is also employed to construct a balanced and comprehensive evaluation dataset, which allows us to effectively assess the model's performance across different tasks and categories. By following this systematic approach, we ensure that the categories covered by our in-house multi-modality SFT data are well-aligned with the taxonomy and representative of real-world usage scenarios.

Main Category	Description	Secondary Category	Tertiary Category
Recognition	This part of the use cases mainly examines the understanding and description ability of large models for image content, which does not require high knowledge reserve and reasoning ability of the model, and some tasks can be completed using traditional machine learning models.	Global Description	Theme Description, Event/Behavior Description, Location/Scene Description, Emotion/Mood Description, Style Recognition, Food Recognition, Others
		Local Description	Pointing Description, Position Description, Person Recognition, Object Attribute Description, Logo Recognition, Counting, Currency Recognition
		OCR and Transcription	Printed Text Transcription, Handwritten Text Transcription, Specified Format Transcription, Specified Language Transcription
Conversion	This type of use case requires the model to be able to describe and recognize image content, and use specific knowledge (e.g., code knowledge, prompt engineering knowledge) to convert image content into another form.	Image to Code	UI to Code, Chart to Code, Photo to SVG/p64 Encoding, Formula to Code, Flowchart to Code
		Image to Text	Image to Prompt, Text Summary, Image-based Creation, Text Interpretation
Analysis	This type of use case requires the model to use specific knowledge and logical ability to make reasonable analysis and understanding based on image content, and describe the image according to instructions.	Data Chart Analysis	Graph Interpretation, Table Interpretation
		Professional Chart Analysis	Circuit Diagram, Flowchart, Map, Music Score, Financial Chart, Floor Plan, Others
		Professional Image Analysis	Sensor Image, Biological and Medical Image, Voiceprint Image, Point Cloud Image
		Encyclopedia Knowledge Analysis	Art and Culture Knowledge, Natural Environment Knowledge, Food/Clothing/Housing/Transportation Related Knowledge, Entertainment Related Knowledge, Historical Knowledge
Commonsense Reasoning	This type of use case mainly tests the model's understanding and mastery of common sense in life, which requires reasoning based on the interpretation and analysis of image content combined with common sense.	Relationship Reasoning	Interpersonal Relationship, Spatial Relationship, Size Relationship, Species Relationship
		Function Reasoning	Hardware Function Reasoning, Software Function Reasoning
		Environment Reasoning	Environment State Analysis, Environment-based Behavior Reasoning, Embodied Intelligence
		Anomaly Reasoning	Identifying Anomalies in Images, Defect Detection, Accident Judgment
		Humor Reasoning	-
		Other Commonsense Reasoning	State Reasoning, Cause Reasoning, Attribute Comparison, Optical Illusion, Fun Games, Intention Interpretation, Behavior Prediction
Logical Reasoning	This type of use case requires the model to combine the understanding of images, comprehensively use domain knowledge and logical reasoning ability to complete corresponding tasks.	Mathematical Reasoning	Algebra and Operation, Plane Geometry, Solid Geometry
		Other Logical Reasoning	Physics, Chemistry, Biology, Code, IQ Questions
Evaluation	This type of use case requires the model to evaluate the image content according to specific criteria.	-	Reality Evaluation, Similarity Evaluation, Aesthetic Evaluation, Open-ended Evaluation, Improvement Suggestions
Multi-graph	This type of use case examines the model's ability to analyze and understand multiple images.	Temporal Sequence Understanding	Event Prediction, Image Sequencing, Behavior Analysis
		Multi-graph Comparison	Attribute Comparison, Image-Text Matching, Finding Associations, Spotting Differences, Image Discrimination
Safety	This type of use case examines the model's performance in terms of safety.	-	Suggestive Questioning, Counterfactual Questioning, Prompt Injection

Table 3 | Our taxonomy for the in-house SFT data. The categories covered by our high-quality in-house multi-modality SFT data are comprehensively represented in this taxonomy.

Furthermore, we include the text-only SFT data employed in DeepSeek-LLM ([DeepSeek-AI, 2024](#)) as part of our joint vision and language SFT data.

3. Approach

3.1. Architecture

Our system contains three modules: a hybrid vision encoder, a vision adaptor, and a language model. We introduce each part in this section.

Hybrid Vision Encoder. We employ SigLIP as the vision encoder to extract high-level semantic feature representations from visual inputs. However, we observe that a single SigLIP encoder struggles to address all real-world questions comprehensively. Vision encoders in the CLIP family, including SigLIP, are primarily designed for semantic visual representations but are challenged by ambiguous encoding, resulting in visually distinct images being encoded as similar due to what is referred to as "CLIP-blind pairs" [Tong et al. \(2024\)](#). Meanwhile, the CLIP family of models is limited by its relatively low-resolution inputs (e.g., 224 x 224, 336 x 336, 384 x 384, 512 x 512), which hinders their ability to handle tasks requiring more detailed low-level features like dense OCR and visual grounding task.

To address these limitations, recent researches ([Lin et al., 2023b; Tong et al., 2024; Wei et al., 2023](#)) have advocated for the integration of additional vision-only self-supervised encoders, to enhance the visual grounding capabilities of multi-modality models. Building upon previous motivations, we additionally utilize a vision-only encoder based on the SAM-B ([Kirillov et al., 2023](#)), a pre-trained ViTDet ([Li et al., 2022](#)) image encoder to process low-level features, which accepts high-resolution 1024 x 1024 image inputs. In addition to the SAM-B encoder, we retain the SigLIP-L vision encoder with low-resolution 384 x 384 image inputs. Consequently, our hybrid vision encoder combines the SAM-B and SigLIP-L encoders, efficiently encoding high-resolution 1024 x 1024 images while preserving both semantic and detailed information. Specifically, a high-resolution SAM-B vision encoder first resizes the image into 1024 x 1024 and results in a 64 x 64 x 256 feature map.

In the case of a high-resolution feature map of size, 64 x 64 x 256 generated by SAM-B, the VL Adaptor initially interpolates it into a size of 96 x 96 x 256. Subsequently, it employs two convolutional layers with a stride of 2, producing a feature map of 24 x 24 x 1024, and reshapes it to 576 x 1024. Alongside this, the low-resolution feature map of size 576 x 1024 generated by SigLIP-L is concatenated with the high-resolution features, resulting in 576 visual tokens with 2048 dimensions. These visual tokens possess a substantial capacity for enhancing high-level semantic visual recognition and low-level visual grounding tasks. Then they undergo GeLU activation and are directed through an embedding layer to establish a connection with the language model.

Vision-Language Adaptor. We employ a two-layer hybrid MLP to bridge the vision encoder and the LLM. Initially, distinct single-layer MLPs are used to process high-resolution features and low-resolution features separately. Subsequently, these features are concatenated along their dimensions and then transformed into the LLM's input space through another layer of MLP.

Language Model. Our language model is built upon DeepSeek LLM ([DeepSeek-AI, 2024](#)) whose micro design largely follows the design of LLaMA ([Touvron et al., 2023a,b](#)), adopting a Pre-Norm structure with RMSNorm ([Zhang and Sennrich, 2019](#)) function and using SwiGLU ([Shazeer, 2020](#)) as the activation function for the Feed-Forward Network (FFN), with an intermediate layer dimension of $\frac{8}{3}d_{model}$. It also incorporates Rotary Embedding ([Su et al.,](#)



Prompt

Is the cyclist on the left or right side of the woman's handbag?



Response

The cyclist is on the left side of the woman's handbag. This can be determined by observing the relative positions of the objects in the image:

1. The woman is holding a handbag that is positioned to her right side, as we view the image.
2. There is a cyclist depicted on the road behind the woman and to her left when looking at the image.
3. The cyclist appears to be moving away from the viewpoint, given their direction and the motion blur effect on their wheels
4. The cyclist is further down the road compared to the woman, which supports the conclusion that they are on the left side of the handbag based on our perspective.

These visual clues confirm that the cyclist is indeed on the left side of the woman's handbag.

Figure 2 | Visualization results. DeepSeek-VL is capable of capturing tiny object and giving organized explanations.

2024) for positional encoding and uses the same tokenizer with DeepSeek-LLM. We introduce a family of DeepSeek-VL models. Given our objective of conducting joint pretraining with multimodal and language, we select an intermediate checkpoint from DeepSeek’s pretrained models to continue pretraining.

Specifically, the DeepSeek-VL-1B model is constructed based on the DeepSeek-LLM-1B model, which underwent training with an approximate corpus of 500 billion text tokens. And the DeepSeek-VL-7B model is developed leveraging the DeepSeek-LLM-7B model trained with an estimated 2 trillion text tokens.

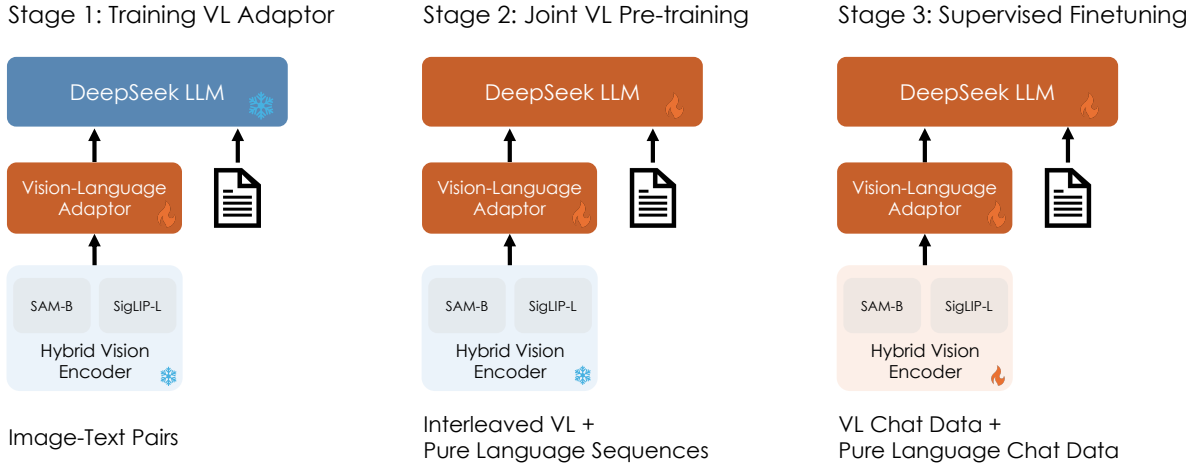


Figure 3 | Our training pipelines consist of three stages. Stage 1 involves training the Vision-Language (VL) adaptor while keeping the hybrid vision encoder and language model fixed. Stage 2 is the crucial part of the joint vision and language pretraining, where both VL adaptor and language model are trainable. Stage 3 is the supervised fine-tuning phase, during which the low-resolution vision encoder SigLIP-L, VL adaptor, and language model will be trained.

3.2. Training Pipelines

We train our DeepSeek-VL in three consecutive stages as shown in Figure 3: vision-language adaptor warmup, joint vision-language pretraining, and supervised fine-tuning. We currently focus on visual understanding capabilities and only calculate the next token prediction loss on the language part.

3.2.1. Stage 1: Training Vision-Language Adaptor

The primary objective of this stage is to establish a conceptual link between visual and linguistic elements within the embedding space, thereby facilitating the comprehensive understanding of depicted entities in the images by the Large Language Model (LLM). Consistent with prior research conducted by LLaVA (Liu et al., 2024b) and Instruct-BLIP (Dai et al., 2023), we adopt a similar approach in which both the vision encoder and the LLM remain frozen during this stage, while solely allowing the trainable parameters within the vision-language adaptor. We utilize a dataset comprising 1.25 million image-text paired captions obtained from ShareGPT4V, along with 2.5 million Document OCR rendering pairs to train the VL adaptor.

Nevertheless, compared to Large Language Models (LLMs), vision-language adaptors (e.g., a 2-layer MLP) have a significantly smaller parameter capacity. This limitation in model capacity restricts the capabilities that can be learned during this stage. A natural question arises: **Can the law of data scaling be effective at this stage?** To address this question, we conducted a simple experiment in Table 8. The results demonstrate that expanding the data scale at this stage does not provide benefits and may even lead to inferior performance. Consequently, we proceed to unfreeze the Large Language Model (LLM) and investigate efficient vision-language pretraining approaches during stage 2.

3.2.2. Stage 2: Joint Vision-Language pretraining

In this stage, we explore effective pretraining strategies which can be considered as an additional stage to enable Large Language Models (LLMs) to comprehend multimodal inputs. We keep the vision encoder frozen and optimize the language model and VL adaptor.

Initially, we attempt to directly train the LLM with multimodal data. However, we find while the metrics for multimodal performance incrementally improved, there is a stark and severe decline in language metrics as illustrated in Figure 4 (Multimodal:Language=100%:0%). This underscores the inherent challenge in directly conducting multimodal pretraining on the foundation of an LLM, revealing a critical trade-off between enhancing multimodal abilities and preserving linguistic proficiency.

We hypothesize that the observed phenomenon stems from two primary factors: firstly, the majority of multimodal corpora, are overly simplistic and exhibit a significant divergence from the complexity and distribution of linguistic data. Secondly, there appears to be a competitive dynamic between multimodal and linguistic modalities, leading to what can be described as catastrophic forgetting of language capabilities within the LLM.

Joint Language-multimodal Training To address this challenge, we devise a straightforward yet effective joint language-multimodal training strategy. During training, we not only engage in multimodal data training but also incorporate a large proportion of language data into the training. This approach aims to balance the training focus, mitigating the adverse effects observed. We conduct experiments on the DeepSeek-VL 1B model in Figure 4 to explore the impact of varying the modality mixing ratios.

The analysis of the graph yields several key conclusions: (1). Integrating language data significantly alleviates the decline in language capabilities, demonstrating a substantial improvement in the model's linguistic performance. (2). The inclusion of language data does not lead to a significant loss in multimodal performance, indicating that the model retains its multimodal processing abilities. (3). The performance of different modalities is strongly correlated with their respective proportions in the training dataset, substantiating the competitive relationship between the two modalities. Ultimately, we opt for a training ratio of language to multimodal data of roughly 7:3 for our final model. This ratio enables the model to maintain its language capabilities while simultaneously achieving better pretraining on multimodal data, effectively balancing the development of both language and multimodal proficiencies.

Scaling Vision-Language Pretraining Nevertheless, the pretraining stage of the model incurs a substantial computational cost, and performing iterations on the 7B model requires an excessive amount of computing power and time. One suitable strategy involves conducting experiments on a smaller model, specifically the 1.3B model, and subsequently scaling it up to the 7B model. Fortunately, we have observed that a significant portion of the outcomes obtained from the 1.3B models can be effectively transferred to the 7B model through the utilization of SFT (e.g., the encoder design). However, during the stage 2 training phase, we have encountered considerable fluctuations in the generative metrics of the 1.3B model, rendering it challenging to supervise the training process effectively. And this has been discussed in [Schaeffer et al. \(2024\)](#), "sharp and unpredictable changes might be induced by the researcher's choice of measurement, even though the model family's per-token error rate changes smoothly, continuously and predictably with increasing scale." Subsequent experiments have led us to identify the root causes of this issue: the limited capacity of the 1.3B model and the absence of SFT data within the training dataset, both of which hinder the model's ability to accurately follow instructions. Even when the model possesses knowledge of the correct options, it struggles to generate them precisely.

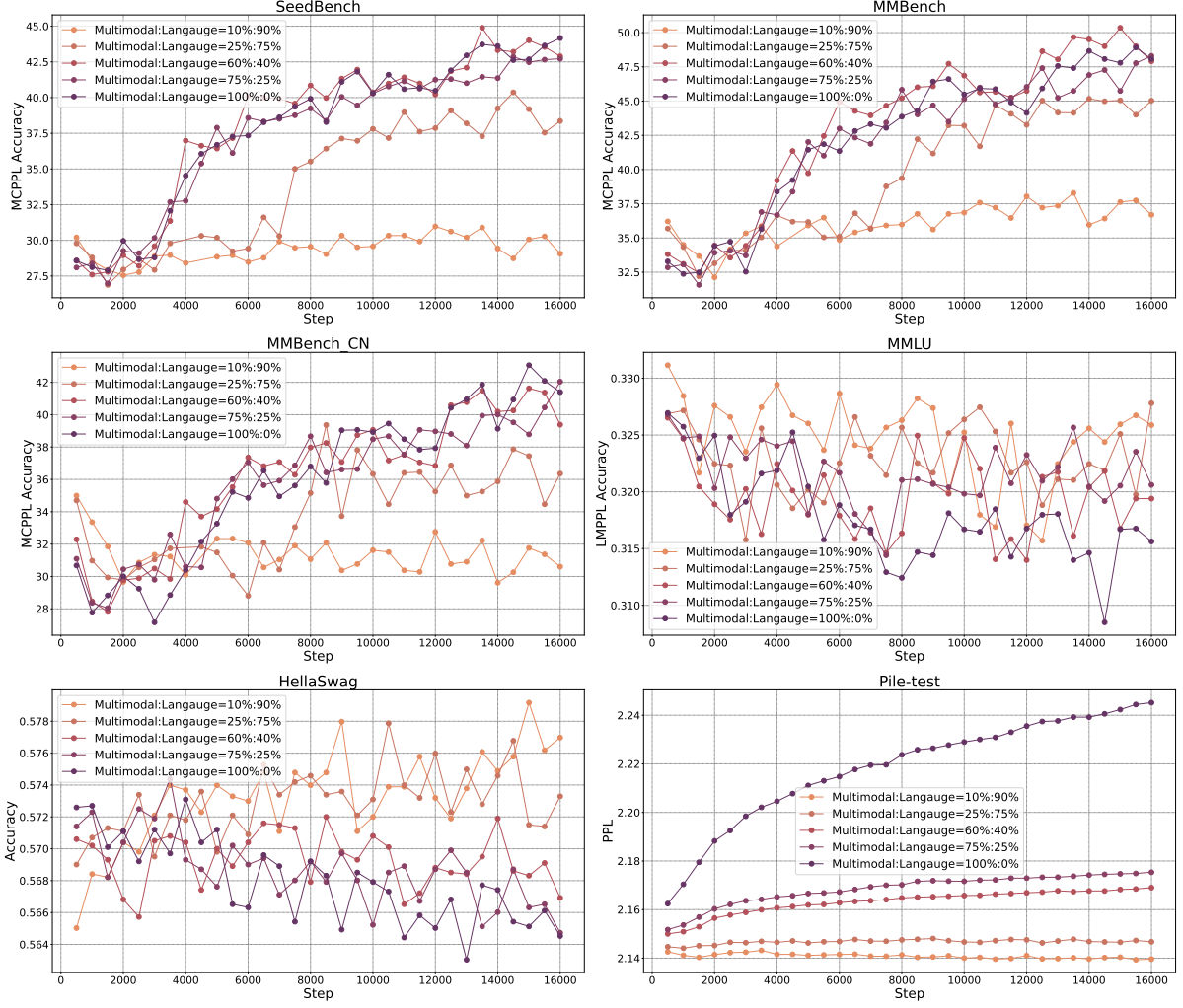


Figure 4 | Comparative performance results on different modality fusion ratio on training stage 2. An excessively large proportion of multimodal data (multimodal:language=100%:0%) leads to significant forgetting of language capabilities in LLMs. A suitable ratio (multimodal:language=70%:30%) can effectively mitigate the issue of language forgetting while simultaneously enhancing the model’s multimodal abilities.

To mitigate these challenges, we adopt a dual-pronged approach. Firstly, we employ the Multi-choice PPL methodology to monitor the model’s progress. This involves inputting not only the prompt and image into the network but also all the answer associated with the question. Subsequently, we calculate the PPL for each answer position (e.g., A, B, C, D) and select the option deemed correct by the model as the final answer. Secondly, we introduce SFT data into the training dataset at a minimal proportion, allowing the model to acquire some proficiency in following instructions. The combination of these two approaches ensures the maintenance of stable training metrics for the 1.3B model and bring better performance after stage3.

3.2.3. Stage 3: Supervised Fine-tuning

In this phase, we finetune the pretrained DeepSeek-VL model with instruction-based fine-tuning to bolster its ability to follow instructions and engage in dialogue, culminating in the creation of the interactive DeepSeek-VL-Chat model. We optimize the language model, VL adaptor, and

 Prompt

Explain the code, step by step.

```

class Solution:
    def longestPalindrome(self, s: str) -> str:
        if len(s) <= 1:
            return s

        Max_Len=1
        Max_Str={0}
        for i in range(len(s)-1):
            for j in range(i+1, len(s)):
                if j-i+1 > Max_Len and s[i:j+1] == s[i:j+1][::-1]:
                    Max_Len = j-i+1
                    Max_Str = s[i:j+1]

        return Max_Str

```

 Response – DeepSeek-VL

The code provided is a Python function that calculates the longest palindrome substring of a given string. The function takes two parameters, which are not defined within this snippet but presumably represent the input strings to be processed.

Here's a step-by-step explanation of how the code works:

1. It defines a helper function called `longestPalindrome` with two arguments, `self` (which is likely a reference to an object or class instance) and `s`. This function returns a value, which we can assume is the length of the longest palindrome substring found in `s`.
2. The main function starts by checking if the length of `s` is less than 1. If true, it immediately returns `s` as there is no palindrome substring for empty or single character strings.
3. Next, it initializes variables `Max_Len` and `Max_Str` to store the maximum length of a palindrome substring found so far.
4. A loop (`for i in range(len(s)-1):`) iterates over all possible starting points of substrings in `s`. For each starting point `i`, another nested loop (`for j in range(i+1, len(s))`) checks whether the substring from index `i` to `j` forms a palindrome. The condition `j - i + 1 > Max_Len` and `s[i:j] == s[i:j][::-1]` ensures that the substring is both longer than the current maximum length and reads the same backward as forward. If this condition is met, it updates `Max_Len` and `Max_Str` with the new maximum length and substring.
5. After iterating through all possible substrings, the function returns `Max_Str`, which contains the longest palindrome substring found.
6. Finally, the line `return Max_Str` indicates that the function will return the result of its computation.

This function uses dynamic programming principles to find the longest palindromic subsequence efficiently by storing intermediate results and avoiding redundant calculations.

Figure 5 | Visualization results. DeepSeek-VL can understand Python code and provide detailed and organized explanations.

hybrid vision encoder with the vision-language SFT data as shown in Table 2, SAM-B remains frozen due to the limited GPU memory. We only supervise answers and special tokens and mask the system and user prompts. To guarantee the model’s comprehensive proficiency in dialogue, we utilize a blend of multimodal data and pure text dialogue data used in DeepSeek-LLM. This approach ensures the model’s versatility across various dialogue scenarios.

3.3. Hyperparameters and Infrastructures

The detailed hyperparameters of all stages are illustrated in Table 4. We train and evaluate our DeepSeek-VL with HAI-LLM (High-flyer, 2023), a lightweight and efficient distributed training framework. Since we use visual encoders to convert images into embedding vectors and then treat image embeddings and text embeddings uniformly, we can easily adapt pipeline parallelism to VL model training: all we need to do is to view visual encoders and text embedding as a single module and take it as the first layer of the resulting model. This very first layer has a complicated model structure and precludes standard tensor parallelism technique, but luckily it requires relatively small computation compared to upper standard transformer blocks. We therefore simply recompute the visual encoder forward pass in all tensor parallel ranks. The existence of visual encoders also leads to non-uniform execution time across model layers, so we re-divide model layers between pipeline parallelism ranks to achieve better load balance and throughput. The upper layers of DeepSeek-VL are exactly the same as those in DeepSeek-LLM. With such minor modification, we can now perform canonical 3D parallelism techniques as in Megatron (Korthikanti et al., 2023; Narayanan et al., 2021; Shoeybi et al., 2019) and overlap computation and communication as in DeepSeek-LLM (DeepSeek-AI, 2024). DeepSeek-VL-7B consumed 5 days on a cluster of 64 nodes, each comprising 8 Nvidia A100 GPUs, while DeepSeek-VL-1B consumed 7 days on a setup involving 16 nodes.

Vision Encoder	DeepSeek-VL 1B			DeepSeek-VL-7B		
	SigLIP			SigLIP+SAM		
Hyperparameters	Stage 1	Stage 2	Stage 3	Stage 1	Stage 2	Stage 3
Learning rate	1.0×10^{-3}	3×10^{-5}	2.0×10^{-5}	1.0×10^{-3}	4.2×10^{-5}	2.0×10^{-5}
LR scheduler	Cosine	Step	Cosine	Cosine	Step	Cosine
Weight decay	0.0	0.0	0.0	0.0	0.0	0.0
Gradient clip	1.0	1.0	1.0	1.0	1.0	1.0
Optimizer	$\text{AdamW}(\beta_1 = 0.9, \beta_2 = 0.95)$			$\text{AdamW}(\beta_1 = 0.9, \beta_2 = 0.95)$		
Warm-up steps	128	2000	256	128	2000	256
Training steps	15000	96000	10000	15000	42000	10000
Batch size	256	1024	256	256	2304	256
Sequence length	512	4096	4096	512	4096	4096
Sequence packing	✗	✓	✗	✗	✓	✗
Pipeline parallelism	✗	✗	✗	✗	✓	✓

Table 4 | Detailed hyperparameters of our DeepSeek-VL.

4. Evaluation

4.1. Public Multimodal Benchmarks Evaluation

We evaluate our models on a series of public benchmarks:

Multimodal comprehensive understanding datasets: MMMU ([Yue et al., 2023](#)), CMMU ([Zhang et al., 2024](#)), MMBench ([Liu et al., 2023a](#)), MMBench-CN ([Liu et al., 2023a](#)), SeedBench ([Li et al., 2023a](#)) and MMV ([Yu et al., 2023b](#)). We compare DeepSeek-VL with competitors on MMB/MMC-dev as current official test download link is no longer active.

Chart/table understanding datasets: OCRBench ([Liu et al., 2023b](#));

Hallucination datasets: POPE ([Li et al., 2023b](#));

Scientific problem datasets: ScienceQA ([Lu et al., 2022a](#)) and MathVista ([Lu et al., 2023](#)).

We apply generation-based evaluation with greedy decoding. The generation-based evaluation here refers to letting the model generate free texts and parsing results from generated texts. The comparative results, as illustrated in Table 5, show that DeepSeek-VL-7B surpasses most open-source models of similar size across a wide range of benchmarks.

DeepSeek-VL outperforms open-source models of similar size in benchmarks such as MMB, MMC, and SEEDbench, even approaching proprietary models (DeepSeek-VL vs. GPT-4V = 70.4 vs. 71.6 on seedbench), demonstrating its powerful natural image comprehension capability. The model also surpasses all open-source models in mathematical logic, but still lags significantly behind proprietary models like GPT-4V (36.1 vs. 47.8 on MathVista). This difference could be attributed to the variance in base model sizes.

Furthermore, as shown in Table 6, DeepSeek-VL-1.3B significantly outperforms models of comparable size. It demonstrates superior performance compared to leading open-source models in the MMB benchmark test, while utilizing only close to half the parameters (1.3B vs. 2.7B), indicating its robust natural image comprehension capability. DeepSeek-VL-1.3B even achieves comparable results to 7B open-source models on MathVista, further validating the powerful logical understanding capabilities of the DeepSeek-VL family.

	LLM	MMMU	CMMMU	MMB	MMC	SEED	OCRB	POPE	MathV	MMVet
Close-source LMMs:										
Gemini Pro	Unk	48.9	-	75.2	74.0	70.7	659	-	45.2	59.2
GPT-4V	Unk	56.8	42.5	75.0	74.7	71.6	659	-	47.8	49.9
Qwen-VL-Plus	Unk	45.2	39.5	66.2	69.6	72.7	-	-	43.3	55.7
Qwen-VL-MAX	Unk	51.4	-	78.1	76.4	72.7	-	-	51.0	61.8
Open-source 13B LMMs:										
LLaVA-1.5	13B	36.4	-	68.2	61.9	68.2	331	85.9	26.4	38.3
VILA	13B	-	-	70.3	64.3	-	-	84.2	-	38.8
LLaVA-Next	13B	36.2	-	70.0	64.4	71.9	-	86.7	35.3	48.4
Open-source 7B LMMs:										
EMU2-Chat	7B	36.3	23.8	63.6	45.9	68.9	-	-	30.0	31.0
Qwen-VL-Chat	7B	37.0	-	60.6	56.7	64.8	-	-	33.8	47.3
CogVLM	7B	37.3	24.8	63.7	53.8	68.8	-	-	34.7	54.5
LLaVA-Next	7B	35.8	-	67.4	60.0	70.2	-	86.5	34.6	43.9
Yi-VL	6B	37.8	35.8	68.2	68.9	67.6	-	-	28.0	31.1
DeepSeek-VL (ours)	7B	36.6	37.9	73.2	72.8	70.4	456	88.1	36.1	41.5

Table 5 | The comparison between different multi-modal models. The top half are proprietary models, while the bottom are open-source models.

	LLM	MMMU	CMMMU	MMB	MMC	SEED	OCRB	POPE	MathV	MMVet
Tiny Model:										
MobileVLM	1.4B	-	-	53.2	-	-	-	84.5	-	-
MobileVLM	2.7B	-	-	59.6	-	-	-	84.9	-	-
MobileVLM V2	1.4B	-	-	59.6	-	-	-	84.3	-	-
MobileVLM V2	2.7B	-	-	63.2	-	-	-	84.7	-	-
LLaVA-Phi	2.7B	-	-	59.5	-	-	-	85.0	-	28.9
DeepSeek-VL (ours)	1.3B	32.2	27.4	64.6	61.3	66.7	409	87.6	31.1	34.8

Table 6 | The comparison between tiny multi-modal models.

4.2. Public Language Benchmarks Evaluation

We evaluate our models on the following public language benchmarks:

Multi-subject multiple-choice datasets including MMLU ([Hendrycks et al., 2020](#)).

Language understanding and reasoning datasets including HellaSwag ([Zellers et al., 2019](#)).

Language modeling datasets including Pile ([Gao et al., 2020](#)).

Math datasets including GSM8K ([Cobbe et al., 2021](#)).

Code datasets including MBPP ([Austin et al., 2021](#)).

Standardized exams including AGIEval ([Zhong et al., 2023](#)).

We apply perplexity-based evaluation to datasets that require answers to be chosen from several options. These datasets include HellaSwag and MMLU. The perplexity-based evaluation here refers to calculating the perplexity of each option and selecting the lowest one as the

	Version Encoder	DeepSeek-VL 1B Chat SigLIP	DeepSeek-VL 7B Chat SigLIP+SAM	DeepSeek-LLM 7B Chat None
Benchmark	HellaSwag	56.0	68.4	68.5
	MMLU	32.5	52.4	49.4
	GSM8K	18.0	55.0	63.0
	MBPP	10.0	35.2	35.2
	AGIEval	14.0	27.8	19.3

Table 7 | The performance on language benchmarks.

model prediction. Perplexity-based evaluation helps to distinguish subtle probability difference between model predictions and avoids discontinuity of exact match style evaluation. We apply generation-based evaluation with greedy decoding for GSM8K and AGIEval. The generation-based evaluation here refers to letting the model generate free texts and parsing results from generated texts. We apply language-modeling-based evaluation for Pile-test, which means calculating the bits-per-byte on the test corpus. And the results are illustrated in Table 7

It can be observed that across the majority of language benchmarks, DeepSeek-VL performs comparably to, or even surpasses, DeepSeek-7B. For instance, it achieves scores of 68.4 vs. 68.5 on HellaSwag, which serves as a general benchmark for evaluating general language ability. DeepSeek-VL outperforms DeepSeek-7B on metrics such as MMLU and AGIEval, indicating that multimodal training methods may even aid in language tasks. Nevertheless, DeepSeek-VL-7B shows a certain degree of decline in mathematics (GSM8K), which suggests that despite efforts to promote harmony between vision and language modalities, there still exists a competitive relationship between them. This could be attributed to the limited model capacity (7B), and larger models might alleviate this issue significantly. Overall, DeepSeek-VL strives to achieve the goal of minimizing declines in language capability while addressing these challenges.

4.3. Human Evaluation

To further explore the capabilities of our DeepSeek-VL, we independently construct a dataset for manual evaluation. This dataset comprises 100 questions, divided into seven categories, each encompassing specific tasks. These categories and tasks are same as our taxonomy for the in-house SFT data, as shown in Table 3. This approach ensures that the tasks we test are universal and encompass the majority of use cases for multimodal models.

Moreover, based on the categories and tasks described in existing reports, we collect similar image materials and developed prompts. The sources for these image materials include royalty-free image communities and photographs taken by the researchers. This methodical collection and prompt formulation process ensures our dataset is both comprehensive and representative of real-world multimodal model applications.

We compare our DeepSeek-VL-7B with InternLM-XComposer2-VL, CogVLM and GPT-4V as shown in Figure 6 (and we also provide visualization results in Appendix A). GPT-4V demonstrates exceptional performance across most dimensions. All open-source models are still far behind GPT-4V in logical reasoning, highlighting the necessity of scaling up the size of Large Language Models (LLMs). DeepSeek-VL-7B achieves better results in overall performance, reaching outcomes close to GPT-4V in Recognition, Conversion, and Commonsense Reasoning.

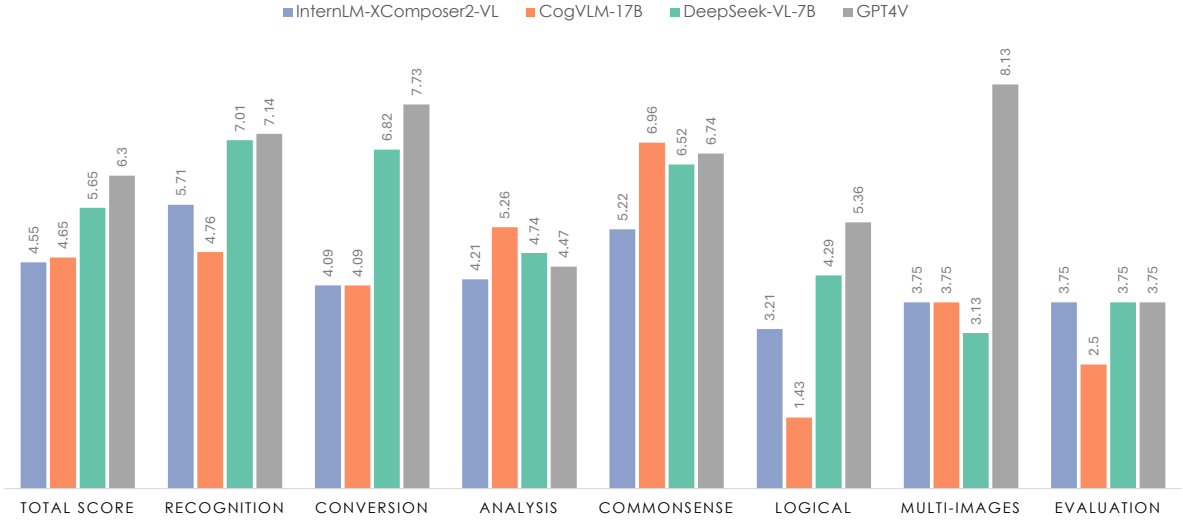


Figure 6 | Human evaluation results on InternLM-XComposer2-VL (Dong et al., 2024), CogVLM (Wang et al., 2023b), DeepSeek-VL and GPT-4V (OpenAI, 2023b).

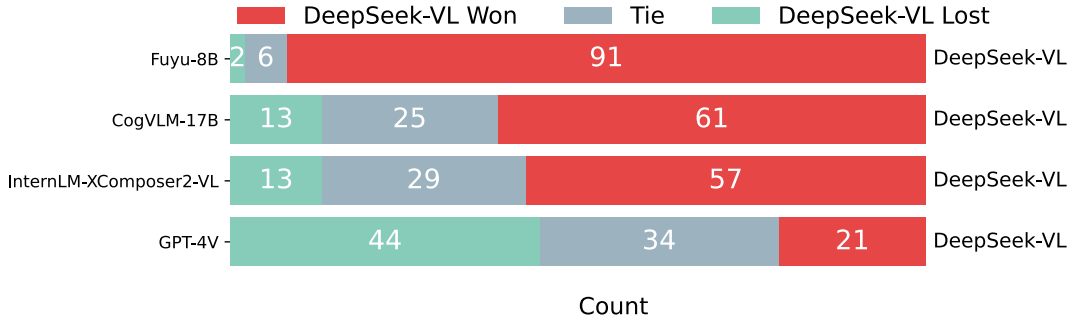


Figure 7 | GPT-4V-based Evaluation Results of DeepSeek-VL vs. Other Models: The chart depicts results from a GPT-4V-based assessment across 99 test samples, demonstrating DeepSeek-VL’s favorable outcomes against both open-source and proprietary models.

In addition, we conduct a comparative assessment using GPT-4V to evaluate the performance of DeepSeek-VL against other models across a set of 99 test samples designed for human evaluation. Following (Zheng et al., 2024), we show GPT-4V the question and the answers from two different models and ask GPT-4V to determine which one is better or declare a tie. The results indicate a preference for DeepSeek-VL’s responses in the majority of cases, as GPT-4V tends to rate the quality of DeepSeek-VL’s answers more favorably. As illustrated in Figure 7, DeepSeek-VL is judged to be superior in over 60% of instances when compared to open-source multimodal models, including Fuyu-8B, CogVLM-17B, and InternLM-XComposer2-VL. Moreover, in comparison with other proprietary models, such as GPT-4V itself, DeepSeek-VL demonstrates comparably exceptional performance.

4.4. Ablation Study

Scale Up Projector Training We expand the dataset for stage 1 (projector warmup) and subsequently apply supervised fine-tuning. The results, depicted in Figure 8, demonstrate that augmenting the training data volume does not enhance performance at this stage. This implies

Stage 1, Training Step	MMB	MMC	SEED	POPE	MMMU	Average
2K	59.0	54.0	61.8	82.3	30.3	57.5
8K	58.0	45.0	58.5	84.9	29.2	55.1
20K	56.0	52.3	59.0	81.7	28.6	55.5
80K	58.1	55.0	58.6	78.6	27.9	55.6

Table 8 | Comparative directly SFT performance results on scaling up stage 1 data. The results demonstrate that expanding the data scale at this stage does not yield benefits, or even results in worse performance.

Stage 1	Stage 2	Stage 3	MMB	MMC	SEED	POPE	MMMU	Average
✓		✓	59.4	54.2	61.4	82.5	29.2	57.4
	✓	✓	63.4	60.5	65.9	87.1	31.8	61.7
✓	✓	✓	64.3	61.3	66.7	87.6	32.2	62.4

Table 9 | Analysis of model performance across training stages.

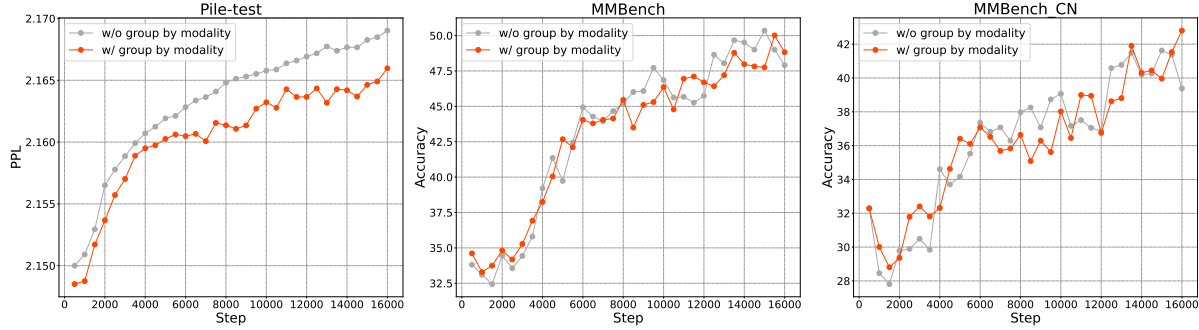


Figure 8 | Comparative analysis of modality warmup on language (Pile-test) and multimodal (MMBench and MMBench_CN) benchmarks demonstrates that modality grouping consistently surpasses the non-grouped modality approach in language tasks, while simultaneously preserving performance on multimodal tasks on training stage 2 (Multimodal:Language=60%:40%).

that the projector’s capacity is inherently constrained, rendering it incapable of capturing the extensive knowledge necessary for multimodal tasks.

Training Stage In Table 9, we examine the contributions of each stage to the model’s performance. It’s evident that combining stage 1, stage 2, and stage 3 yields significantly better results across all metrics compared to combining stage 1 and stage 3 alone, demonstrating the effectiveness of multimodal pretraining. Additionally, the combination of stage 2 and stage 3 still slightly lags behind the combined performance of stage 1, stage 2, and stage 3, indicating that vision-language adaptor warmup stage remains meaningful.

Modality Group Training When mixing language and multimodal data, we observe that directly blending them at the batch level significantly reduces training efficiency. This inefficiency arises because each batch gradient backpropagation process waits for the slowest sample to complete. As a result, the predominantly faster-to-process pure language data ends up waiting for the multimodal samples to finish, leading to a decrease in overall training efficiency.

To address this issue, we experiment with grouping different modalities of data at each global

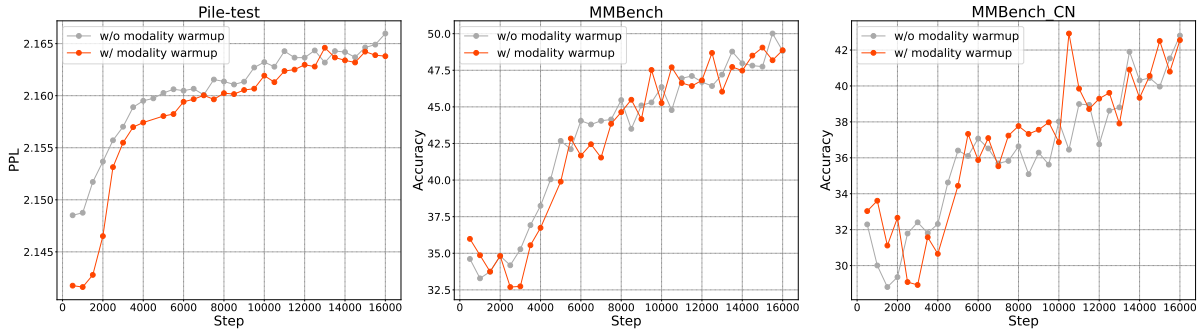


Figure 9 | Comparative performance results on language (Pile-test) and multimodal (MMBench and MMBench_CN) benchmarks for modality warmup. Modality warmup consistently matches or surpasses the performance of approaches without modality warmup across all evaluated tasks on training stage 2 (Multimodal:Language=60%:40%).

step, sampling distinct modalities separately. This approach involves organizing the training data so that batches are composed either entirely of language data or entirely of multimodal data at different training steps, rather than mixing them within the same batch.

The results are shown in Figure 8, we observe that this method does not compromise the model’s performance while enhancing the model’s training efficiency by 20%. This strategy effectively circumvents the bottleneck caused by the disparate processing times between modalities, optimizing the training workflow.

Modality Warmup Considering that our approach involves multimodal training on the foundation of a language model, directly mixing multimodal data in a fixed proportion from the outset can destabilize the model. To counteract this issue, we propose a simple yet effective modality warm-up strategy. Initially, we set the language data ratio to 1, and then gradually decrease it to the target ratio for the final model training (e.g., 0.7).

Our experiments, as illustrated in Figure 9, demonstrate that this strategy effectively prevents a significant decline in language capabilities at the beginning of training, while also yielding comparatively superior outcomes in the final phases for both the language and multimodal domains. This gradual adaptation enables the model to more seamlessly adjust to the incorporation of multimodal data, thereby improving overall training stability and performance.

Vision Encoder Selection In order to better acquire and utilize image information, we compare the training loss of different vision encoders under our training settings except for reducing training steps of stage 2 to 8000 for efficiency. As illustrated in Figure 10, the incorporation of vision-only self-supervised encoders has been found to significantly enhance performance on training loss. To more effectively process high-resolution images, our research ultimately adopts a hybrid vision encoder strategy, combining SigLIP with SAM for our model’s implementation.

Vision-Language Adaptor Design To improve the efficiency of extracting information from the visual encoder while adhering to current token length constraints, adjustments can be made to the Vision-Language adaptor in two main ways: the method used to combine visual features and the design of the MLP adaptor.

Previous studies (Tong et al., 2024) have indicated that combining visual features along the sequence dimension can lead to better model performance, although this comes with the trade-off of increased computational requirements due to a longer sequence of visual feature tokens. As demonstrated in the top section of Table 10, reducing the sequence length by stacking

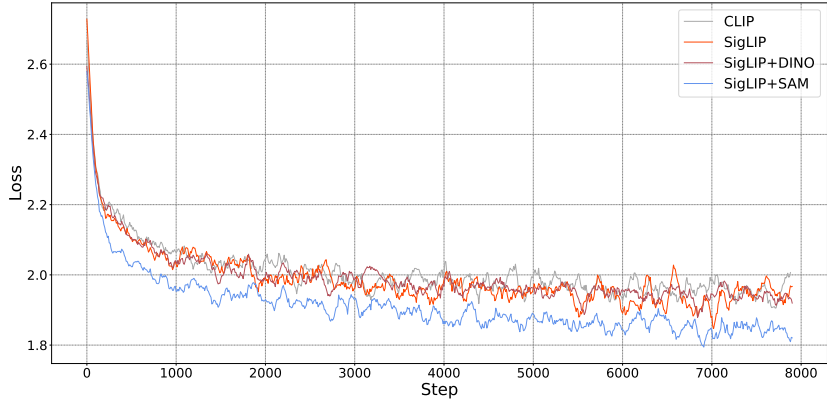


Figure 10 | Comparative analysis of different vision encoders on training losses in stage 2.

Architecture	MMB	MMC	SEED	POPE	ScienceQA	MMMU	OCRB	Average
Sequence Concatenation:								
Token Pooling - W	61.2	<u>59.6</u>	61.6	86.5	57.7	<u>31.6</u>	304	55.5
Token Pooling - H	59.9	58.3	61.6	83.8	55.0	32.0	291	54.2
Embedding Concatenation:								
Hybrid MLP	<u>61.7</u>	60.1	<u>62.9</u>	87.8	<u>56.6</u>	31.3	<u>309</u>	55.9
Shared MLP	62.0	58.9	62.5	<u>86.6</u>	54.7	30.2	318	55.2
Separate MLP	57.5	58.7	63.1	86.5	<u>56.6</u>	29.0	299	54.5

Table 10 | Comparison of different adaptor architectures using SigLIP and SAM as hybrid vision encoder, Hybrid MLP are used for sequence concatenation experiments. **Bolded** entries represent the best results, while underlined entries denote the second-best results. For calculating the average score, we divide the OCRBench by the total number of questions.

visual features along the image’s width or height dimensions before sequence concatenation, in order to keep the sequence length constant, does not achieve better results compared to simply merging them along the embedding dimension in most metrics. In terms of the adaptor architecture, employing separate MLP adaptors for each vision feature encoder allows for more precise adjustments to the specific values and distribution patterns of visual features, facilitating smoother model training. Conversely, using a shared MLP adaptor for different vision encoders contributes to adequate feature fusion. We adopt a mixed strategy and report stable and improved performance, as outlined in the lower section of Table 10.

5. Conclusion, Limitation, and Future Work

In this technical report, we have introduced DeepSeek-VL, a series of Multimodal Large Language Models, available in scales of 1.3B and 6.7B parameters. This report has unveiled the limitations inherent in the predominant projector-based pretraining methodologies, setting the stage for the innovative approach adopted by DeepSeek-VL. By prioritizing a joint vision and language (VL) pretraining phase, DeepSeek-VL transcends traditional models by ensuring that the integration of multimodal data does not compromise the linguistic capabilities of the Large Language Models (LLMs). This is achieved through a strategic warm-up data ratio and the introduction of a hybrid vision encoder, which together enable the efficient processing of

high-resolution images without losing sight of semantic richness.

The incorporation of a hybrid vision encoder, capable of handling 1024 x 1024 images within a constrained token budget, underscores our commitment to preserving the nuanced details and semantic integrity across diverse tasks. As a result, DeepSeek-VL emerges as a pioneering model that not only meets but exceeds the standards set by generalist models in its class. It showcases exceptional performance across a wide range of visually-centric benchmarks while sustaining formidable proficiency in language-centric evaluations.

In making DeepSeek-VL publicly available, we aim to catalyze further innovation and exploration within the research community, providing a robust foundation upon which future studies can build. This gesture of openness is intended to facilitate the collective advancement of our understanding and capabilities in handling multimodal data.

Looking ahead, we are excited to announce plans to scale up DeepSeek-VL to larger sizes, incorporating Mixture of Experts (MoE) technology. This forthcoming expansion promises to further enhance the model's efficiency and effectiveness, opening up new horizons for research and application in the field of AI.

References

- 01-ai. Yi-34B vision language model. <https://huggingface.co/01-ai/Yi-VL-34B>, 2024.
- Abi. Screenshot to code. <https://github.com/abi/screenshot-to-code>, 2024.
- Anna’s Archive. Anna’s archive. <https://annas-archive.org/>, 2024.
- Anthropic. Introducing Claude, 2023. URL <https://www.anthropic.com/index/introducing-claude>.
- J. Austin, A. Odena, M. Nye, M. Bosma, H. Michalewski, D. Dohan, E. Jiang, C. Cai, M. Terry, Q. Le, et al. Program synthesis with large language models. [arXiv preprint arXiv:2108.07732](https://arxiv.org/abs/2108.07732), 2021.
- J. Bai, S. Bai, S. Yang, S. Wang, S. Tan, P. Wang, J. Lin, C. Zhou, and J. Zhou. Qwen-vl: A versatile vision-language model for understanding, localization, text reading, and beyond. [arXiv preprint arXiv:2308.12966](https://arxiv.org/abs/2308.12966), 2023.
- R. Bavishi, E. Elsen, C. Hawthorne, M. Nye, A. Odena, A. Soman, and S. Taşırlar. Introducing our multimodal models, 2023. URL <https://www.adept.ai/blog/fuyu-8b>.
- L. Blecher. Latex-ocr. GitHub repository, 2024. URL <https://github.com/lukas-blecher/LaTeX-OCR>.
- L. Blecher, G. Cucurull, T. Scialom, and R. Stojnic. Nougar: Neural optical understanding for academic documents. [arXiv preprint arXiv:2308.13418](https://arxiv.org/abs/2308.13418), 2023.
- A. Burns, K. Srinivasan, J. Ainslie, G. Brown, B. A. Plummer, K. Saenko, J. Ni, and M. Guo. A suite of generative tasks for multi-level multimodal webpage understanding. In [The 2023 Conference on Empirical Methods in Natural Language Processing \(EMNLP\)](https://openreview.net/forum?id=rwcLHjtUmn), 2023. URL <https://openreview.net/forum?id=rwcLHjtUmn>.
- J. Carter. Textocr-gpt4v. <https://huggingface.co/datasets/jimmycarter/textocr-gpt4v>, 2024.

- L. Chen, J. Li, X. Dong, P. Zhang, C. He, J. Wang, F. Zhao, and D. Lin. Sharegpt4v: Improving large multi-modal models with better captions. [arXiv preprint arXiv:2311.12793](#), 2023.
- C. K. Chng, Y. Liu, Y. Sun, C. C. Ng, C. Luo, Z. Ni, C. Fang, S. Zhang, J. Han, E. Ding, et al. Icdar2019 robust reading challenge on arbitrary-shaped text-rrc-art. In [2019 International Conference on Document Analysis and Recognition \(ICDAR\)](#), pages 1571–1576. IEEE, 2019.
- K. Cobbe, V. Kosaraju, M. Bavarian, M. Chen, H. Jun, L. Kaiser, M. Plappert, J. Tworek, J. Hilton, R. Nakano, et al. Training verifiers to solve math word problems. [arXiv preprint arXiv:2110.14168](#), 2021.
- W. Dai, J. Li, D. Li, A. M. H. Tiong, J. Zhao, W. Wang, B. Li, P. Fung, and S. Hoi. Instructblip: Towards general-purpose vision-language models with instruction tuning, 2023.
- DeepSeek-AI. Deepseek llm: Scaling open-source language models with longtermism. [arXiv preprint arXiv:2401.02954](#), 2024. URL <https://github.com/deepseek-ai/DeepSeek-LM>.
- X. Dong, P. Zhang, Y. Zang, Y. Cao, B. Wang, L. Ouyang, X. Wei, S. Zhang, H. Duan, M. Cao, et al. Internlm-xcomposer2: Mastering free-form text-image composition and comprehension in vision-language large model. [arXiv preprint arXiv:2401.16420](#), 2024.
- echo840. Detailed caption dataset. https://huggingface.co/datasets/echo840/Detailed_Caption, 2024.
- W. Foundation. Wikimedia downloads. URL <https://dumps.wikimedia.org>.
- J. Gao, R. Pi, J. Zhang, J. Ye, W. Zhong, Y. Wang, L. Hong, J. Han, H. Xu, Z. Li, et al. G-llava: Solving geometric problem with multi-modal large language model. [arXiv preprint arXiv:2312.11370](#), 2023.
- L. Gao, S. Biderman, S. Black, L. Golding, T. Hoppe, C. Foster, J. Phang, H. He, A. Thite, N. Nabeshima, et al. The Pile: An 800GB dataset of diverse text for language modeling. [arXiv preprint arXiv:2101.00027](#), 2020.
- Google. An important next step on our AI journey, 2023. URL <https://blog.google/technology/ai/bard-google-ai-search-updates/>.
- D. Hendrycks, C. Burns, S. Basart, A. Zou, M. Mazeika, D. Song, and J. Steinhardt. Measuring massive multitask language understanding. [arXiv preprint arXiv:2009.03300](#), 2020.
- High-flyer. Hai-llm: 高效且轻量的大模型训练工具, 2023. URL <https://www.high-flyer.cn/en/blog/hai-llm>.
- Y.-C. Hsiao, F. Zubach, M. Wang, et al. Screenqa: Large-scale question-answer pairs over mobile app screenshots. [arXiv preprint arXiv:2209.08199](#), 2022.
- A. Hu, Y. Shi, H. Xu, J. Ye, Q. Ye, M. Yan, C. Li, Q. Qian, J. Zhang, and F. Huang. mplug-paperowl: Scientific diagram analysis with the multimodal large language model. [arXiv preprint arXiv:2311.18248](#), 2023.
- HuggingFaceM4. Websight dataset. <https://huggingface.co/datasets/HuggingFaceM4/WebSight>, 2024.

- S. Kantharaj, R. T. Leong, X. Lin, A. Masry, M. Thakkar, E. Hoque, and S. Joty. Chart-to-text: A large-scale benchmark for chart summarization. In S. Muresan, P. Nakov, and A. Villavicencio, editors, *Proceedings of the 60th Annual Meeting of the Association for Computational Linguistics (Volume 1: Long Papers)*, pages 4005–4023, Dublin, Ireland, May 2022. Association for Computational Linguistics. doi: 10.18653/v1/2022.acl-long.277. URL <https://aclanthology.org/2022.acl-long.277>.
- A. Kirillov, E. Mintun, N. Ravi, H. Mao, C. Rolland, L. Gustafson, T. Xiao, S. Whitehead, A. C. Berg, W.-Y. Lo, et al. Segment anything. *arXiv preprint arXiv:2304.02643*, 2023.
- D. Kocetkov, R. Li, L. B. Allal, J. Li, C. Mou, C. M. Ferrandis, Y. Jernite, M. Mitchell, S. Hughes, T. Wolf, D. Bahdanau, L. von Werra, and H. de Vries. The stack: 3 tb of permissively licensed source code. In *Transactions on Machine Learning Research*, 2023.
- V. A. Korthikanti, J. Casper, S. Lym, L. McAfee, M. Andersch, M. Shoeybi, and B. Catanzaro. Reducing activation recomputation in large transformer models. *Proceedings of Machine Learning and Systems*, 5, 2023.
- I. Krylov, S. Nosov, and V. Sovrasov. Open images v5 text annotation and yet another mask text spotter. In *Asian Conference on Machine Learning*, pages 379–389. PMLR, 2021.
- A. Kulkarni and J. Truelson. wkhtmltopdf. <https://wkhtmltopdf.org/>. Project maintained by Ashish Kulkarni, originally created by Jakob Truelson. Accessed: 2024-02-22.
- LAION. Gpt-4v dataset. <https://huggingface.co/datasets/laion/gpt4v-dataset>, 2023.
- B. Li, R. Wang, G. Wang, Y. Ge, Y. Ge, and Y. Shan. Seed-bench: Benchmarking multimodal llms with generative comprehension. *arXiv preprint arXiv:2307.16125*, 2023a.
- S. Li and N. Tajbakhsh. Scigraphqa: A large-scale synthetic multi-turn question-answering dataset for scientific graphs, 2023.
- Y. Li, G. Li, L. He, J. Zheng, H. Li, and Z. Guan. Widget captioning: Generating natural language description for mobile user interface elements. *arXiv preprint arXiv:2010.04295*, 2020.
- Y. Li, H. Mao, R. Girshick, and K. He. Exploring plain vision transformer backbones for object detection. In *European Conference on Computer Vision*, pages 280–296. Springer, 2022.
- Y. Li, Y. Du, K. Zhou, J. Wang, W. X. Zhao, and J.-R. Wen. Evaluating object hallucination in large vision-language models. *arXiv preprint arXiv:2305.10355*, 2023b.
- J. Lin, H. Yin, W. Ping, Y. Lu, P. Molchanov, A. Tao, H. Mao, J. Kautz, M. Shoeybi, and S. Han. Vila: On pre-training for visual language models. *arXiv preprint arXiv:2312.07533*, 2023a.
- Z. Lin, C. Liu, R. Zhang, P. Gao, L. Qiu, H. Xiao, H. Qiu, C. Lin, W. Shao, K. Chen, et al. Sphinx: The joint mixing of weights, tasks, and visual embeddings for multi-modal large language models. *arXiv preprint arXiv:2311.07575*, 2023b.
- F. Liu, F. Piccinno, S. Krichene, C. Pang, K. Lee, M. Joshi, Y. Altun, N. Collier, and J. M. Eisenschlos. Matcha: Enhancing visual language pretraining with math reasoning and chart derendering. *arXiv preprint arXiv:2212.09662*, 2022a.
- H. Liu, C. Li, Y. Li, B. Li, Y. Zhang, S. Shen, and Y. J. Lee. Llava-next: Improved reasoning, ocr, and world knowledge, January 2024a. URL <https://llava-vl.github.io/blog/2024-01-30-llava-next/>.

- H. Liu, C. Li, Q. Wu, and Y. J. Lee. Visual instruction tuning. *Advances in neural information processing systems*, 36, 2024b.
- Y. Liu, G. Zhu, B. Zhu, Q. Song, G. Ge, H. Chen, G. Qiao, R. Peng, L. Wu, and J. Wang. Taisu: A 166m large-scale high-quality dataset for chinese vision-language pre-training. In S. Koyejo, S. Mohamed, A. Agarwal, D. Belgrave, K. Cho, and A. Oh, editors, *Advances in Neural Information Processing Systems*, volume 35, pages 16705–16717. Curran Associates, Inc., 2022b. URL https://proceedings.neurips.cc/paper_files/paper/2022/file/6a386d703b50f1cf1f61ab02a15967bb-Paper-Datasets_and_Benchmarks.pdf.
- Y. Liu, H. Duan, Y. Zhang, B. Li, S. Zhang, W. Zhao, Y. Yuan, J. Wang, C. He, Z. Liu, et al. Mmbench: Is your multi-modal model an all-around player? *arXiv preprint arXiv:2307.06281*, 2023a.
- Y. Liu, Z. Li, H. Li, W. Yu, M. Huang, D. Peng, M. Liu, M. Chen, C. Li, L. Jin, et al. On the hidden mystery of ocr in large multimodal models. *arXiv preprint arXiv:2305.07895*, 2023b.
- S. Long, S. Qin, D. Panteleev, A. Bissacco, Y. Fujii, and M. Raptis. Towards end-to-end unified scene text detection and layout analysis. In *Proceedings of the IEEE/CVF Conference on Computer Vision and Pattern Recognition*, 2022.
- P. Lu, L. Qiu, J. Chen, T. Xia, Y. Zhao, W. Zhang, Z. Yu, X. Liang, and S.-C. Zhu. Iconqa: A new benchmark for abstract diagram understanding and visual language reasoning. *arXiv preprint arXiv:2110.13214*, 2021.
- P. Lu, S. Mishra, T. Xia, L. Qiu, K.-W. Chang, S.-C. Zhu, O. Tafjord, P. Clark, and A. Kalyan. Learn to explain: Multimodal reasoning via thought chains for science question answering. In *The 36th Conference on Neural Information Processing Systems (NeurIPS)*, 2022a.
- P. Lu, S. Mishra, T. Xia, L. Qiu, K.-W. Chang, S.-C. Zhu, O. Tafjord, P. Clark, and A. Kalyan. Learn to explain: Multimodal reasoning via thought chains for science question answering. *Advances in Neural Information Processing Systems*, 35:2507–2521, 2022b.
- P. Lu, H. Bansal, T. Xia, J. Liu, C. Li, H. Hajishirzi, H. Cheng, K.-W. Chang, M. Galley, and J. Gao. Mathvista: Evaluating mathematical reasoning of foundation models in visual contexts. *arXiv preprint arXiv:2310.02255*, 2023.
- J. Mao, J. Huang, A. Toshev, O. Camburu, A. L. Yuille, and K. Murphy. Generation and comprehension of unambiguous object descriptions. In *Proceedings of the IEEE conference on computer vision and pattern recognition*, pages 11–20, 2016.
- A. Masry, P. Kavehzadeh, X. L. Do, E. Hoque, and S. Joty. Unichart: A universal vision-language pretrained model for chart comprehension and reasoning. *arXiv preprint arXiv:2305.14761*, 2023.
- D. Narayanan, M. Shoeybi, J. Casper, P. LeGresley, M. Patwary, V. Korthikanti, D. Vainbrand, P. Kashinkunti, J. Bernauer, B. Catanzaro, et al. Efficient large-scale language model training on gpu clusters using megatron-lm. In *Proceedings of the International Conference for High Performance Computing, Networking, Storage and Analysis*, pages 1–15, 2021.
- N. Nayef, F. Yin, I. Bizid, H. Choi, Y. Feng, D. Karatzas, Z. Luo, U. Pal, C. Rigaud, J. Chazalon, et al. Icdar2017 robust reading challenge on multi-lingual scene text detection and script identification-rrc-mlt. In *2017 14th IAPR international conference on document analysis and recognition (ICDAR)*, volume 1, pages 1454–1459. IEEE, 2017.

- OpenAI. Chatgpt: Optimizing language models for dialogue. 2022. URL <https://openai.com/blog/chatgpt>.
- OpenAI. GPT-4 technical report. *arXiv*, 2023a.
- R. OpenAI. Gpt-4v(ision) system card. 2023b.
- J. A. Rodriguez, D. Vazquez, I. Laradji, M. Pedersoli, and P. Rodriguez. Ocr-vqgan: Tampering text-within-image generation. In *Proceedings of the IEEE/CVF Winter Conference on Applications of Computer Vision*, pages 3689–3698, 2023.
- R. Schaeffer, B. Miranda, and S. Koyejo. Are emergent abilities of large language models a mirage? *Advances in Neural Information Processing Systems*, 36, 2024.
- N. Shazeer. Glu variants improve transformer. *arXiv preprint arXiv:2002.05202*, 2020.
- B. Shi, C. Yao, M. Liao, M. Yang, P. Xu, L. Cui, S. Belongie, S. Lu, and X. Bai. Icdar2017 competition on reading chinese text in the wild (rctw-17). In *2017 14th iapr international conference on document analysis and recognition (ICDAR)*, volume 1, pages 1429–1434. IEEE, 2017.
- M. Shoeybi, M. Patwary, R. Puri, P. LeGresley, J. Casper, and B. Catanzaro. Megatron-lm: Training multi-billion parameter language models using model parallelism. *arXiv preprint arXiv:1909.08053*, 2019.
- A. Singh, G. Pang, M. Toh, J. Huang, W. Galuba, and T. Hassner. Textocr: Towards large-scale end-to-end reasoning for arbitrary-shaped scene text. In *Proceedings of the IEEE/CVF conference on computer vision and pattern recognition*, pages 8802–8812, 2021.
- J. Su, M. Ahmed, Y. Lu, S. Pan, W. Bo, and Y. Liu. Roformer: Enhanced transformer with rotary position embedding. *Neurocomputing*, 568:127063, 2024.
- Q. Sun, Q. Yu, Y. Cui, F. Zhang, X. Zhang, Y. Wang, H. Gao, J. Liu, T. Huang, and X. Wang. Generative pretraining in multimodality. *arXiv preprint arXiv:2307.05222*, 2023.
- Y. Sun, Z. Ni, C.-K. Chng, Y. Liu, C. Luo, C. C. Ng, J. Han, E. Ding, J. Liu, D. Karatzas, et al. Icdar 2019 competition on large-scale street view text with partial labeling-rrc-lsvt. In *2019 International Conference on Document Analysis and Recognition (ICDAR)*, pages 1557–1562. IEEE, 2019.
- G. Team, R. Anil, S. Borgeaud, Y. Wu, J.-B. Alayrac, J. Yu, R. Soricut, J. Schalkwyk, A. M. Dai, A. Hauth, et al. Gemini: a family of highly capable multimodal models. *arXiv preprint arXiv:2312.11805*, 2023.
- S. Tong, Z. Liu, Y. Zhai, Y. Ma, Y. LeCun, and S. Xie. Eyes wide shut? exploring the visual shortcomings of multimodal llms. *arXiv preprint arXiv:2401.06209*, 2024.
- H. Touvron, T. Lavril, G. Izacard, X. Martinet, M.-A. Lachaux, T. Lacroix, B. Rozière, N. Goyal, E. Hambro, F. Azhar, et al. LLaMA: Open and efficient foundation language models. *arXiv preprint arXiv:2302.13971*, 2023a.
- H. Touvron, L. Martin, K. Stone, P. Albert, A. Almahairi, Y. Babaei, N. Bashlykov, S. Batra, P. Bhargava, S. Bhosale, D. Bikel, L. Blecher, C. Canton-Ferrer, M. Chen, G. Cucurull, D. Esiobu, J. Fernandes, J. Fu, W. Fu, B. Fuller, C. Gao, V. Goswami, N. Goyal, A. Hartshorn, S. Hosseini, R. Hou, H. Inan, M. Kardas, V. Kerkez, M. Khabsa, I. Kloumann, A. Korenev, P. S. Koura, M. Lachaux, T. Lavril, J. Lee, D. Liskovich, Y. Lu, Y. Mao, X. Martinet, T. Mihaylov, P. Mishra,

- I. Molybog, Y. Nie, A. Poulton, J. Reizenstein, R. Rungta, K. Saladi, A. Schelten, R. Silva, E. M. Smith, R. Subramanian, X. E. Tan, B. Tang, R. Taylor, A. Williams, J. X. Kuan, P. Xu, Z. Yan, I. Zarov, Y. Zhang, A. Fan, M. Kambadur, S. Narang, A. Rodriguez, R. Stojnic, S. Edunov, and T. Scialom. Llama 2: Open foundation and fine-tuned chat models. *CoRR*, abs/2307.09288, 2023b. doi: 10.48550/arXiv.2307.09288. URL <https://doi.org/10.48550/arXiv.2307.09288>.
- A. Veit, T. Matera, L. Neumann, J. Matas, and S. Belongie. Coco-text: Dataset and benchmark for text detection and recognition in natural images. *arXiv preprint arXiv:1601.07140*, 2016.
- B. Wang, G. Li, X. Zhou, Z. Chen, T. Grossman, and Y. Li. Screen2words: Automatic mobile ui summarization with multimodal learning. In *The 34th Annual ACM Symposium on User Interface Software and Technology*, pages 498–510, 2021.
- J. Wang, L. Meng, Z. Weng, B. He, Z. Wu, and Y.-G. Jiang. To see is to believe: Prompting gpt-4v for better visual instruction tuning. *arXiv preprint arXiv:2311.07574*, 2023a.
- W. Wang, Q. Lv, W. Yu, W. Hong, J. Qi, Y. Wang, J. Ji, Z. Yang, L. Zhao, X. Song, et al. Cogvilm: Visual expert for pretrained language models. *arXiv preprint arXiv:2311.03079*, 2023b.
- H. Wei, L. Kong, J. Chen, L. Zhao, Z. Ge, J. Yang, J. Sun, C. Han, and X. Zhang. Vary: Scaling up the vision vocabulary for large vision-language models. *arXiv preprint arXiv:2312.06109*, 2023.
- Y. Yang, A. Panagopoulou, Q. Lyu, L. Zhang, M. Yatskar, and C. Callison-Burch. Visual goal-step inference using wikihow. *arXiv preprint arXiv:2104.05845*, 2021.
- J. Ye, A. Hu, H. Xu, Q. Ye, M. Yan, G. Xu, C. Li, J. Tian, Q. Qian, J. Zhang, et al. Ureader: Universal ocr-free visually-situated language understanding with multimodal large language model. *arXiv preprint arXiv:2310.05126*, 2023.
- Q. Yu, Q. Sun, X. Zhang, Y. Cui, F. Zhang, Y. Cao, X. Wang, and J. Liu. Capsfusion: Rethinking image-text data at scale. *arXiv preprint arXiv:2310.20550*, 2023a.
- W. Yu, Z. Yang, L. Li, J. Wang, K. Lin, Z. Liu, X. Wang, and L. Wang. Mm-vet: Evaluating large multimodal models for integrated capabilities. *arXiv preprint arXiv:2308.02490*, 2023b.
- X. Yue, Y. Ni, K. Zhang, T. Zheng, R. Liu, G. Zhang, S. Stevens, D. Jiang, W. Ren, Y. Sun, et al. Mmmu: A massive multi-discipline multimodal understanding and reasoning benchmark for expert agi. *arXiv preprint arXiv:2311.16502*, 2023.
- R. Zellers, A. Holtzman, Y. Bisk, A. Farhadi, and Y. Choi. HellaSwag: Can a machine really finish your sentence? In A. Korhonen, D. R. Traum, and L. Màrquez, editors, *Proceedings of the 57th Conference of the Association for Computational Linguistics, ACL 2019, Florence, Italy, July 28- August 2, 2019, Volume 1: Long Papers*, pages 4791–4800. Association for Computational Linguistics, 2019. doi: 10.18653/v1/p19-1472. URL <https://doi.org/10.18653/v1/p19-1472>.
- B. Zhang and R. Sennrich. Root mean square layer normalization. *Advances in Neural Information Processing Systems*, 32, 2019.
- G. Zhang, X. Du, B. Chen, Y. Liang, T. Luo, T. Zheng, K. Zhu, Y. Cheng, C. Xu, S. Guo, et al. Cmmmu: A chinese massive multi-discipline multimodal understanding benchmark. *arXiv preprint arXiv:2401.11944*, 2024.

- R. Zhang, Y. Zhou, Q. Jiang, Q. Song, N. Li, K. Zhou, L. Wang, D. Wang, M. Liao, M. Yang, et al. Icdar 2019 robust reading challenge on reading chinese text on signboard. In 2019 international conference on document analysis and recognition (ICDAR), pages 1577–1581. IEEE, 2019.
- Y. Zhang, L. Gueguen, I. Zharkov, P. Zhang, K. Seifert, and B. Kadlec. Uber-text: A large-scale dataset for optical character recognition from street-level imagery. In SUNw: Scene Understanding Workshop - CVPR 2017, Hawaii, U.S.A., 2017. URL <http://sunw.csail.mit.edu/abstract/uberText.pdf>.
- L. Zheng, W.-L. Chiang, Y. Sheng, S. Zhuang, Z. Wu, Y. Zhuang, Z. Lin, Z. Li, D. Li, E. Xing, et al. Judging llm-as-a-judge with mt-bench and chatbot arena. Advances in Neural Information Processing Systems, 36, 2024.
- W. Zhong, R. Cui, Y. Guo, Y. Liang, S. Lu, Y. Wang, A. Saied, W. Chen, and N. Duan. AGIEval: A human-centric benchmark for evaluating foundation models. CoRR, abs/2304.06364, 2023. doi: 10.48550/arXiv.2304.06364. URL <https://doi.org/10.48550/arXiv.2304.06364>.
- W. Zhu, J. Hessel, A. Awadalla, S. Y. Gadre, J. Dodge, A. Fang, Y. Yu, L. Schmidt, W. Y. Wang, and Y. Choi. Multimodal c4: An open, billion-scale corpus of images interleaved with text. Advances in Neural Information Processing Systems, 36, 2024.

A. Appendix

Prompt

将这段流程图转换为python程序

```

when green flag clicked
set [my variable v] to [pick random (1) to (10)]
repeat (1)
  ask [Guess a number between 1 and 10] and wait
  if [answer] > [my variable] then
    say [Too high!] for (1) seconds
  else
    if [answer] < [my variable] then
      say [Too low!] for (1) seconds
  end
end
say [You got it!]

```

Response – DeepSeek-VL

这段流程图展示了一个使用Python编程语言编写的猜数字游戏。游戏的目的是玩家猜测一个在1到10之间的随机数，如果猜对了，游戏就会结束并显示“你赢了！”（You got it!）。如果玩家的猜测超过了或低于这个范围，游戏会提示“太高了！”（Too high!）或“太低了！”（Too low!），然后玩家可以再次尝试。

根据流程图的描述，我们可以将这个游戏实现为以下Python代码：

```

import random

# 设置变量来存储猜测和答案
guess = None
answer = random.randint(1, 10)

while guess != answer:
    # 询问玩家猜测一个1到10之间的数字
    print("请猜测一个1到10之间的数字。")
    guess = int(input())

    if guess < 1 or guess > 10:
        print("你的猜测超出了范围。请重新猜测。")
    elif guess > answer:
        print("太高了！")
    else:
        print("太低了！")
else:
    print("你赢了！")

```

在这个程序中，我们使用了random.randint()函数来生成一个1到10之间的随机整数作为答案。然后，我们进入一个循环，直到玩家的猜测等于答案为止。在每次猜测后，我们会检查玩家的猜测是否在范围内，以及它是否等于答案。如果是，我们就打印出“你赢了！”；如果不是，我们就打印出“太高了！”或“太低了！”，然后让玩家再次猜测。一旦玩家的猜测等于答案，游戏就结束了。

Response – Open-source Model 1

sorry, as a language model AI, I cannot process image into any other content.

Response – Open-source Model 2

当然！这里有一个 Python 代码片段可以复制流程图：```python

```

def guess_number():
    while True:
        number = random.randint(1, 10)
        print(f'Guess a number between 1 and 10 and wait:', number)
        answer = input()
        if answer == number:
            print('太高了！等待1秒')
            continue
        elif answer < number:
            print('太低了！等待1秒')
            continue
        else:
            print('你猜中了！')
            break

```

Figure 11 | Visualization results. DeepSeek-VL can understand children’s programming diagrams from the real world and provide detailed and organized explanations.

Prompt

Explain the image.

(b) Different proportions of multi-step stages

Response – DeepSeek-VL

The image is a line graph that compares the performance of two different learning rate schedulers, namely the Multi Step Learning Rate Scheduler and the Cosine Learning Rate Scheduler. The x-axis represents the number of processed tokens in billions, ranging from 0 to 100 billion. The y-axis represents the training loss, which ranges from 2.0 to 3.0.

The blue line represents the Multi Step Learning Rate Scheduler with three steps of increasing rates: (80% + 10% + 10%). This line starts at a high point near 3.0 on the y-axis when the number of processed tokens is 0 billion, indicating a higher initial loss. As the number of processed tokens increases, this line shows a steep decline in training loss, suggesting rapid improvement in model performance as more data is processed. However, after approximately 40 billion processed tokens, the line begins to level off, indicating diminishing returns on further processing.

The orange line represents the Cosine Learning Rate Scheduler. It also starts at a high point near 3.0 when the number of processed tokens is 0 billion but has a much smoother descent than the blue line. This suggests a slower but steady decrease in training loss as more tokens are processed. After around 60 billion processed tokens, this line levels off as well, similar to the blue line.

Both lines show a general trend of decreasing training loss as the number of processed tokens increases, indicating improved model performance over time. However, the Multi Step Learning Rate Scheduler appears to achieve lower losses more quickly compared to the Cosine Learning Rate Scheduler, especially in the early stages of processing tokens.

Response – Open-source Model 1

Line 1 expresses the number of tokens, following a nonlinear trend. Line 2 starts at value 80, then is decreasing and increases by 10% until reaching a value where it then increases by 10%, before it flattens out. Line 3 also starts in increasing part, then has some constant decreases between different points, and after that express an increasing part.

Response – Open-source Model 2

The image displays a line graph comparing the training losses of two different learning rates schedulers: the Multi Step Learning Rate Scheduler ($80\% + 10\% = 10\%$) and the Cosine Learning Rate Scheduler. The y-axis represents the training loss in terms of billions, ranging from approximately 2.2 to 3.0. The x-axis represents the number of processed tokens, with a range from 0 to 100. The Multi Step Learning Rate Scheduler's line is blue, showing a sharp decline initially and then stabilizing. The Cosine Learning Rate Scheduler's line is orange, showing a more gradual decline.

Prompt

Help me find the bug.

```
def find_max_in_sequence(sequence):
    if not sequence:
        return None

    max_value = sequence[1]

    for num in sequence:
        if num > max_value:
            max_value = num

    return max_value
```

Response – DeepSeek-VL

The image shows a piece of code written in Python, which is intended to find the maximum value in a sequence. The function definition starts with "def" indicating that this is a new function being defined. The name of the function is "find_max_in_sequence".
The first line checks if the input is not a sequence; if it is, the function returns None. This is an important check because functions should only operate on sequences (like lists or tuples) and not other types of data structures. If the input is not a sequence, the function will return no result, which can be useful for handling invalid inputs.
Next, there's a statement defining what a sequence is: `max_value = sequence [1]`. This seems incorrect as it assigns the index 1 to `max_value` instead of the actual element at position 1 in the sequence.
Then we have a loop that iterates over each number in the sequence. It uses an "if" condition to check whether the current number (num) is greater than the current maximum value (`max_value`). If true, it updates `max_value` to be equal to num. This part of the code appears correct, as it correctly compares each number against the current maximum value and updates the maximum when necessary.
Finally, after the loop ends, the function returns the updated `max_value`, which contains the maximum value found in the sequence.
Based on the visual clues provided by the code snippet, the bug lies in the assignment of `max_value` where it incorrectly assigns the index 1 rather than the value at that index in the sequence. The corrected version would look like this: `max_value = sequence[0]`.
This error could potentially lead to unexpected results if the sequence has more than one element, as the function might fail to find the maximum value due to the wrong assignment of `max_value`.

Response – Open-source Model 1

The function name in the code is "find_max_in_sequence", but it has not actually been called as the condition of the if-statement checks for 'not sequence' instead of 'if not sequence'. The actual line where the function should be called is missing from the provided code.

Response – Open-source Model 2

The bug in the code is that the condition for returning 'None' is set to 'if not sequence', which is incorrect. The correct condition should be 'if not max_value', to ensure that the function returns 'None' when the sequence is not found or when the max value is not found within the sequence.

Figure 12 | Visualization results. DeepSeek-VL has strong understanding capabilities for code and charts in the real world.

Prompt

What coin is that?



Response – DeepSeek-VL

The coin is a 10 Baht coin from Thailand.

Prompt

请根据这张图片，创作一首七言绝句



Response – DeepSeek-VL

山川暮色映斜阳，
林间雪覆寒意长。
孤树影斜人未归，
一抹残霞照断肠。

Prompt

图中的角色是哪家公司的？



Response – DeepSeek-VL

图中的角色是miHoYo (米哈游) 公司的。这家公司以其开发的手机游戏《原神》而闻名，该游戏中的角色设计风格与图片中角色的风格相似。此外，图片中的角色穿着和武器设计也符合miHoYo游戏的特征。

Prompt

图像中的角色来自游戏公司“原神”。

Response – Open-source Model 1

图像中的角色来自游戏公司“原神”。

Prompt

这张图片展示的角色是日本Square Enix公司旗下的一款游戏《最终幻想14》中的角色。

Response – Open-source Model 2

answering does not require reading text in the image

Figure 13 | Visualization results. DeepSeek-VL possesses extensive knowledge of the real world.

32

Prompt

Convert it to markdown table.

Table I. Comparison of our dataset with other released datasets.

Dataset	#Frames					#A
	Total	Training	Testing	Regularity	Irregularity	
Our Dataset	317,398	274,515	42,883	300,308	17,090	
CUHK Avenue	30,652	15,328	15,324	26,832	3,820	
UCSD Ped2	4,560	2,550	2,010	2,924	1,636	
UCSD Ped1	14,000	6,800	7,200	9,995	4,005	
Subway Entrance	136,524	20,000	116,524	134,124	2,400	
Subway Exit	72,401	7,500	64,901	71,681	720	



Response – DeepSeek-VL

Here is the image content converted into a markdown table:

Dataset	Total Frames	Training Frames	Testing Frames	Regularity	Irregularity	#A
Our Dataset	317,998	274,515	42,883	300,308	17,090	-
CUHK Avenue	30,652	15,328	15,324	3,820	-	-
UCSD Ped2	4,560	2,550	2,010	2,924	1,656	-
UCSD Ped1	14,000	6,800	7,200	9,955	4,005	-
Subway Entrance	136,524	20,000	116,524	134,124	2,400	-
Subway Exit	72,401	7,500	64,901	71,681	720	-

Please note that the "A" column in the original table seems to be empty or not fully visible in the image provided.



Response – Open-source Model 1

Dataset	#Frames	Total	Training	Testing	Regularity	Irregularity
CUHK Avenue	30,652	37,398	27,515	42,988	300,308	17,090
UCSD Perf2	4,560	2,550	2,010	2,924	2,924	1,656
UCSD Perf1	14,000	6,800	7,200	9,955	4,005	4,005
Subway Entrance	136,524	20,000	116,524	134,124	2,400	1,7567
Subway Exit	72,491	7,500	64,901	71,681	720	645



Response – Open-source Model 2

Dataset	Total	Training	Testing	Regularity	Irregularity
Our Dataset	317,398	274,515	42,883	300,308	17,990
CUHK Avenue	30.652	15,328	15,324	26,832	3,820
UCSD Ped2	4.560	2,550	2,010	2,924	1,636
UCSD Ped1	14,000	6,800	7,200	9,995	4,005
Subway Entrance	136,524	20,000	11,624	13,424	2,400
Subway Exit	74,401	7,500	64,901	71,681	720

Figure 14 | Visualization results. DeepSeek-VL is capable of accurately reading the contents of real-world tables.